Monetary Policy Effectiveness in Times of Crisis: Evidence from the Euro Area Money Market

Paola Donati*

15 January 2010

Abstract

This paper investigates the risk premia embedded in the three-month Euribor - which is a benchmark for pricing assets denominated in euros - and gauges how such risk premia have been affected by the monetary and liquidity policy measures carried out by the ECB, from end 2005 to end 2009. First, the magnitude of the risk premia is measured by contrasting the three-month Euribor with its secured counterpart, namely the three-month Eurepo. Then, the Euribor-Eurepo spread is decomposed into: 1) a compensation for counterparty credit risk, 2) a compensation for liquidity risk, and 3) a compensation for systemic risk.

In order to estimate, in real time, also how persistent has been the effect of each ECB's measure on the risk premia, the paper introduces a multivariate frequency decomposition method cast in the unobserved component framework. To measure whether the effectiveness of monetary policy has increased during the financial crisis compared with the past, the parameters of the employed state-space model are allowed to vary with time. The frequency decompositions, along with the estimation of the model, are performed with a low-, band-pass filter, which also corrects for the performance degradation due to model simplifications and misspecifications and data measurement errors.

JEL classification: B41, C22, E43, E58, G01

Keywords: Turmoil; Money Market Rates; Monetary Policy; Model Misspecification; Frequency Decomposition; Non-Gaussian Filtering; State-Space Model;

*European Central Bank, Directorate General Research, Kaiserstrasse 29, D-60311 Frankfurt am Main, Germany. Email: paola.donati@ecb.europa.eu. This paper was previously circulated with the title "The Effect of Conventional and Unconventional Monetary Policy on the Money Market Spreads in the Euro Area". I would like to thank Nuno Cassola, Francesco Donati, Gabriel Fagan, Domenico Giannone, Philipp Hartmann, Cornelia Holthausen, Angela Maddaloni, David Marques-Ibanez, Francesco Papadia, José Luis Peydró, Loriana Pelizzon, Jens Tapking, and the participants at the ECB workshop on *Challenges to monetary policy implementation beyond the financial market turbulence* and at the 20^{th} $(EC)^2$ Conference on *Real Time Econometrics* for helpful comments and suggestions. Initial contributions by Cristina Picillo and Stefano Nardelli are thankfully acknowledged. The empirical analysis of this study greatly benefited from the tools included in EicasLab: I would like to thank the programmers of this computing environment for their assistance. The views expressed in this paper are my own and they do not necessarily reflect those of the European Central Bank or the Eurosystem.

1 Introduction

The global financial crisis that erupted in August 2007 has been characterized by unprecedented and persistent rises in interest rates on *unsecured* interbank lending – as measured by the Libor (London Interbank Offered Rate) and, in the euro area, by the Euribor (Euro Interbank Offered Rate) – due to a surge in their embedded risk premia.

Banks lending cash to other banks in unsecured money market transactions are fully exposed to *counterparty credit risk*, that is to the risk of incurring into financial losses if the cash borrowers become insolvent; to funding and market *liquidity risk*, that is to the risk that the cash borrowers default or repay their debt with a delay because, albeit potentially solvent, they face specific funding liquidity problems or because no trade takes place in the unsecured money market; and to the *systemic risk* of a seizing-up of the financial system, for example prompted by the failure of large and interconnected institutions as it notably happened in the autumn of 2008.[1]

As emphasized by Caballero and Krishnamurthy (2008), the recent surge observed in Libor and Euribor levels reflected a sharp and unexpected rise in uncertainty, because, following the correction in U.S. house prices that started in 2006, the market suddenly realized that it did not know how to value the structured credit products backed by U.S. subprime mortgages traded in several developed economies in the years preceding the crisis. The subsequent steady fall in the prices of subprime related assets, and then the demise of interconnected financial institutions, induced a worldwide reassessment of risk. Under these conditions, the increase in the demand for liquidity by banks hit by negative shocks combined with general liquidity hoarding for precautionary reasons, producing the breakdown of interbank markets.[2] The banks that kept on trading, demanded a high compensation to lend each other uncollateralized funds beyond overnight to account for the potentially high funding costs they would incur into should they themselves need to raise cash in the money market when the loans they had granted had not yet matured, as shown for the euro area by Eisenschmidt and Tapking (2009). Subsequently, asymmetric information on the potential solvency of counterparty financial institutions fostered adverse selection, and then a further rise in interbank interest rate levels to compensate for credit risk, so that more banks, finding it too expensive to borrow, dropped out of the market contributing to its paralysis, as explained by Heider, Hoerova and Holthausen (2009).[3]

[1] See e.g. Trichet (2009) "Systemic Risk", Distinguished Lecture in Economics and Public Policy, University of Cambridge, 10 December; de Bandt, O., and P. Hartmann (2000), "Systemic Risk: A Survey", ECB Working Paper no 14; de Bandt, O., P. Hartmann and J. Peydro (2009), "Systemic Risk in Banking: An Update", forthcoming ECB Working Paper; Berger, A., P. Molyneux and J. Wilson (eds.), Oxford Handbook of Banking, Oxford University Press, 2009, and the references therein.

[2] A review of the events characterizing the crisis is provided in Adrian and Shin (2008), "Liquidity and Leverage", Staff Report no. 328, Federal Reserve Bank of New York; Allen and Carletti (2009), "An Overview of the Crisis: Causes, Consequences and Solutions", forthcoming in *International Review of Finance*; Brunnermeier (2009), "Deciphering the Liquidity and Credit Crunch 2007-08", *Journal of Economic Perspectives*, 23, 77-100.

[3] For studies on the problem of asymmetric information see also Bhattacharya and Gale (1987), "Preference Shocks, Liquidity and Central Bank Poliy", in Barnett and Singleton (Eds), New Approaches to Monetary Economics,

Under conditions of inefficient liquidity provision by the market, central bank interventions are needed to address the liquidity risk because banks cannot hedge against idiosyncratic and aggregate liquidity shocks, due to the incompleteness of the asset market, as explained by Allen, Carletti and Gale (2009). In the euro area, as a consequence of the dislocations caused by the crisis, many banks increasingly relied on central bank money to finance their liquidity needs, accepting also to pay a liquidity premium to participate into the European Central Bank (ECB) tenders, as reported by Cassola and Morana (2008).

To help reduce liquidity risk premia, and the risk that potentially solvent banks became insolvent because of a shortage of liquidity with potential systemic repercussions, in 2007 the ECB increased the frequency of its open market operations with a three-month maturity, in 2008 it introduced refinancing operations with one- and six-month maturity, and in 2009 it carried out three operations with one-year maturity. Starting from 15 October 2008, to preserve the functioning of the monetary policy transmission mechanism, the ECB pursued also an *enhanced credit support policy* whereby it carried out all the refinancing operations with a fixed rate tender procedure with full allotment at the policy rate, and it temporary expanded the list of eligible collateral. At the same time, in response to the deterioration in the economic outlook in the euro area, the ECB rapidly reduced the monetary policy rate level from 4.25 percent to 1.00 percent (Trichet 2009a, 2009b, and ECB 2008, 2009).

This paper makes three points. The first consists in the measure, carried out in real time, of the effect produced by the ECB's monetary and liquidity policies on the risk premia embedded in the three-month Euribor, which plays an important role in the transmission mechanism of monetary policy in the euro area, and it is a widely used benchmark for pricing assets and loans denominated in euros. The second point concerns the theory of multivariate frequency decomposition. In particular, to estimate how *persistent* the corrective actions taken by the ECB have been, we introduce a method to perform real-time multivariate frequency decompositions cast in the unobserved component framework advocated by Harvey (1985), Watson (1986), Clark (1987), among others, and more recently by Perron and Wada (2009). To measure whether the effectiveness of monetary and liquidity policy has increased during the financial crisis compared with the past, the parameters of the employed state-space model are allowed to vary with time. Following the procedure proposed by Donati and Donati (2008), the frequency decomposition is carried out in real time, using a low-, band-pass filter, which through its recursions also corrects for the performance degradation caused by model simplifications and possible misspecifications as well as data measurement errors. The third point consists in the decomposition of the risk premia included in the Euribor into a compensation for credit, liquidity, and systemic risk.

Cambridge University Press, Cambridge, pp. 69-88; Flannery (1996), "Financial Crises, Payment System Problems and Discount Window Lending", *Journal of Money, Credit and Banking*, 28, pp. 804-24; Frexias and Jorge (2008), "The Role of Interbank Markets in Monetary Policy: A Model with Rationing", Working Paper, Universitat Pompeu Fabra.

This study is related to work by Nobili (2009), who also investigates the risk premia embedded in the Euribor but without evaluating the persistence of the risk components and without directly measuring the effect produced by the ECB's policies, and to work by Artuç and Demiralp (2009), McAndrews, Sarkar, and Wang (2008), Fleming, Hrung, and Keane (2009), Taylor and Williams (2009), Wu (2008), and Christensen, Lopez and Rudebusch (2009) who investigate the effects on secured and unsecured US money market rates entailed during the turmoil by the measures taken by the Federal Reserve.

The paper is organized as follows. Section 2 reviews the measures taken by the ECB after the emergence of the crisis. Section 3 presents the data. Sections 4 and 5 decompose into frequencies the time series of interest to extract the long-, medium-, and short-run shocks explaining their dynamics, using a univariate frequency decomposition model. Section 6 introduces a multivariate frequency decomposition model gauging how the shocks extracted from the time series of interest affected the dynamics of the risk premia embedded in the Euribor. Section 7 presents the results on the effectiveness of the ECB's measures. Section 8 concludes.

2 Conventional and Unconventional Monetary Policy Measures

The ECB separates the role of the monetary policy decisions on the interest rate level — which determine the monetary policy stance and are taken with the objective of maintaining price stability in the euro area over the medium-term — from the role of the liquidity operations steered towards the implementation of the selected monetary policy stance without imposing any distortion. This separation principle has been respected in the first phase of the turmoil up to mid-October 2008, but in the second phase of the crisis unconventional liquidity measures have been adopted with the specific aim of influencing the prevailing short-term interest rate levels.[4] The adopted measures relevant for this study are reviewed in the next two sections.

2.1 Conventional Measures and the First Phase of the Crisis

From the emergence of the turmoil in the euro area, on 9 August 2007, until 15 October 2008, in order to offset the shortage of liquidity in the money market and to neutralize to the possible extent the factors driving the EONIA (Euro Overnight Index Average) away from the policy rate level, the ECB adopted a number of conventional measures including:

1. The introduction, on 22 August 2007 and 12 September 2007, of two supplementary reverse transaction, collateral-based, long-term refinancing operations with a three-month maturity

[4]See also Bini Smaghi L. (2009), "Conventional and Unconventional Monetary Policy", keynote lecture delivered at the International Center for Monetary and Banking Studies (ICMB), Geneva, 28 April 2009.

(*LTRO3m*) to facilitate the solution of maturity mismatches between the assets and liabilities of some banks.[5]

2. The introduction, on 8 October 2007, of a *frontloading* policy whereby the liquidity weekly allotted at the main refinancing operations (*MRO*)[6] was increased above the benchmark[7] early in the maintenance period and reduced thereafter in order to leave the average liquidity allotted in any maintenance period unchanged. This policy had the objective of accommodating the uncertainty-driven preference of many banks to fulfill their reserve requirements relatively early in the reserve maintenance period.[8]

3. Starting from end-November 2007, the increase above the neutral benchmark of the liquidity allotted at the *MRO*, and the lengthening of the maturity of the penultimate *MRO* of 2007 to two weeks,[9] in order to meet year-end rises in liquidity demand.

4. The introduction, on 3 April 2008, of reverse transaction, collateral-based, long-term refinancing operations with a six-month maturity (*LTRO6m*), and on 29 September 2008 the introduction of reverse transaction, collateral-based, special term refinancing operations (*STRO*) with about one month maturity matching the length of the reserve maintenance period

Despite the introduction of supplementary liquidity-providing measures, during this initial phase of the turmoil (Cecchetti and Disyatat, 2009), the ECB maintained essentially unchanged at about EUR 455 billion the average outstanding level of liquidity temporarily lent to the banking system. Yet, the ECB altered, by lengthening it, the average maturity of central bank money borrowing. Whereas in the first eight months of 2007 the *LTRO3m* accounted for about 33% of the total net lending to credit institutions, the share of the *LTROs* as a whole edged up to an average 62% from August 2007 to mid October 2008. The liquidity allotted at the *MRO* was reduced accordingly.

[5] In normal times, the LTRO3m are executed on a monthly basis, typically in the form of variable tenders, with allotment amounts preset by the ECB.

[6] The main refinancing operations (*MRO*) are the most important open market operations through which liquidity (i.e. banks' current account holdings with the ECB) is lent for a week to bank counterparties against eligible collateral. The *MRO* are reverse transaction operations used to steer the EONIA close to the policy rate, to manage the liquidity situation in the market and to signal the stance of monetary policy. In normal times, the ECB presets the allotted amount at a level close to the benchmark, and the *MRO* are executed through variable rate tenders in which banks bid both the amount of liquidity they wish to borrow against collateral and the interest rate at which they wish to enter into the transaction for up to ten different interest rates. The minimum bid rate on the *MRO* is the monetary policy rate set by the ECB.

[7] The benchmark refers to the estimates made by the ECB of the liquidity which banks need both to meet their reserve requirements and to satisfy their liquidity needs (for example the demand for banknotes) during each maintenance period.

[8] These requirements need to be complied with on average over each maintenance period, which lasts about one month.

[9] At that *MRO* the ECB satisfied all bids at or above the weighted average rate of the previous *MRO*, resulting in an allotment sizeably above the benchmark, as explained in ECB (2008).

2.2 Unconventional Measures and the Second Phase of the Crisis

The financial crisis further intensified in September 2008, shortly after the filing for bankruptcy by Lehman Brothers: a dramatic loss of confidence affected market participants, the money market liquidity virtually dried up, the money market spreads reached all time highs and the short-term rates sizeably departed from the ECB policy rate. Starting from 15 October 2008, to safeguard both the functioning of the money market and the transmission mechanism of monetary policy, the ECB adopted an *enhanced credit support* policy (Trichet, 2009a) whereby *unconventional* measures have directly influenced both the cost and availability of liquidity to banks. These include:

1. The temporary extension of the list of assets eligible as collateral at the *MRO* and the *LTROs* thereby making it easier for banks to borrow central bank money.

2. The introduction of a fixed rate tender procedure with full allotment at the policy rate for all the *MRO* and the *LTROs* in order to let banks borrow as much weekly and term collateralized liquidity as they bid without charging any term premium.

3. The increase of the frequency of the long-term refinancing operations by carrying out two *LTRO3m*, one *LTRO6m*, and one *STRO* every month.

4. On 25 June 2009, the introduction of reverse transaction, collateral-based, long-term refinancing operations with a one-year maturity (*LTRO1Y*), carried out with a fixed rate full allotment tender procedure, in order to lengthen banks' liquidity plannings and to reduce the surrounding uncertainty.

Moreover, in response to rapidly receding inflationary pressures and the worsening of the economic outlook, starting from 15 October 2008 the ECB progressively reduced the monetary policy rate (*MPR*), from 4.25 percent to 1.00 percent.

The change in the tender procedures and the increase in the number of open market operations have been accompanied by an increase in the total volume of outstanding liquidity: net lending to credit institutions peaked at EUR 678 billion in early December 2008, up from EUR 525 billion at the end of December 2007. The expansion of the central bank balance sheet has characterized the second phase of the crisis.

3 Data Description

To measure the risk premia embedded in the Euribor with a three-month maturity, we contrast the Euribor with the benchmark provided by the Eurepo with a three-month maturity. The difference between the two rates (*Spread*) is measured in basis points and it is taken at a working day frequency over the period from 3 October 2005 to 30 November 2009 (1086 observations).

The three-month Euribor is the rate at which prime banks in the euro area offer to lend *unsecured* funds denominated in euros for a three month period to other euro area prime banks.[10] The three-month Eurepo is the rate at which one prime bank offers to lend, in the euro area and worldwide, *secured* funds in euros to another prime bank against the exchange of Eurepo General Collateral (GC).[11] The Euribor and the Eurepo react essentially to the same economic developments, including the actual and expected changes in the monetary policy stance. Moreover, both contracts involve an initial exchange of cash which is paid back at maturity.

The difference between the two contracts is that lenders in Euribor transactions are fully exposed to the *counterparty credit risk* that the cash borrowers become insolvent, to the *liquidity risk* that the cash borrowers face funding liquidity problems, e.g. in liquidating their positions, or that there is no possibility to trade assets in the unsecured money market at the moment of the settlement, e.g. because the market has become illiquid, and to the *systemic risk* of a seizing-up of the financial system.

Lenders in Eurepo transactions, by receiving in exchange GC that consists primarily of high quality government securities, are protected from counterparty credit risk,[12] but remain exposed to liquidity risk and to systemic risk depending on the prevailing conditions in the repo and in the GC markets. As a result, the Euribor-Eurepo spread includes the compensation demanded by the market for bearing credit risk in unsecured interbank transactions, as well as the liquidity and systemic risk premia embedded in the Euribor and the Eurepo, which do not cancel out when computing the spread (Michaud and Upper, 2008).

To measure the credit risk component of the Euribor-Eurepo spread, we employ the cost of buying an insurance against the risk of default by a borrowing bank on its debt as measured by credit default swap (CDS) spreads. Specifically, we consider the iTraxx financial senior index for Europe (*iTraxxFS*), measured in basis points, provided by Bloomberg, which contains 25 senior subordination financial names for the five year credit default swap contract. Although for the purpose of this study this index has the drawback of not matching money market rates maturities and of not necessarily matching the financial names reporting Euribor and Eurepo quotes,[13] this

[10] The Euribor levels are daily non-binding quotes, which need not stem from actual transactions, collected from a panel of about 40 euro area banks with the highest volume of business in the euro area money market. They are published daily at 11 a.m. (CET).

[11] The Eurepo levels are also daily quotes collected from a panel of about 40 representative banks and they are also published daily at 11 a.m. (CET).

[12] Furthermore, during the recent crisis euro area collateralized repo rates experienced less disruptions than repo denominated in other currencies (Hördahl and King, 2008), their spread vis-a-vis overnight interest swap rates did not increase significantly, and banks have not become reluctant to lend also term collateralized funds to other banks (Eisenschmidt and Tapking, 2009).

[13] On the other side, Michaud and Upper (2008) found evidence that banks with higher CDS premia did not appear to quote Euribor levels significantly higher than banks with lower credit risk, thereby loosening the direct link between the CDS spreads on the banks in the Euribor panel and the quoted Euribor. Instead, it seems plausible that the writedowns and individual bank losses moving the widely monitored iTraxx financial senior index, being interpreted as signals on bank credit quality, get also reflected in the Euribor rates.

index has the important advantage of not being affected by the liquidity conditions prevailing in the money market. In addition it is a benchmark, it is tradable, its price is set by market demand and its constituents are updated every six months.

Due to the lack of data on market liquidity conditions,[14] the liquidity risk premia are extracted from the Euribor-Eurepo spread using the monetary and liquidity measures taken by the ECB. In particular, the effect on the spread related to changes observed in the *iTraxxFS*, in the outstanding volumes of central bank liquidity, and in the monetary policy rate, are estimated with a system of simultaneous equations. The compensation for risk that cannot be explained by the *iTraxxFS*, and that is directly affected by the ECB's measures, is ascribed to liquidity risk.[15]

Finally, we ascribe to systemic risk the share of the risk premia embedded in the Euribor which cannot be explained by changes in the CDS spreads or in the ECB's measures. This means that the shocks triggering the demand for such risk compensation originate outside the euro area and due to the interconnectedness of the global financial system they increase also the risk premium embedded in the Euribor. The generating shocks may also have a domestic origin and have magnitude outsizing the corrective effect of the measures taken by the ECB and by the EU fiscal authorities (the effect of the latter being captured by the *iTraxxFS*). Finally, the events generating the systemic risk premia embedded in the Euribor may reflect a worldwide market stance or bias, as for example the general underpricing of risk that occurred before the eruption of the crisis (in this case the systemic risk premia are negative).

The ECB's conventional and unconventional measures considered in this study include the changes, measured in percentage points, in the monetary policy rate, and the changes in the outstanding liquidity volumes, measured in EUR millions, due to the MRO and all the LTROs implemented up to 30 November 2009. The data are taken from the website of the ECB.

4 The Univariate Frequency Decomposition Model

We begin by performing the frequency decomposition of each variable considered in this study using the unobserved components approach proposed by Donati and Donati (2008). Such approach presumes that the dynamics of a time series, denoted $z(t)$, is driven by a number of independent forces whose effects manifest themselves at different time horizons. In particular, here we consider three broad, mutually disjoint, sets of shocks, which need not be normally distributed as in Perron and Wada (2009): 1) *long-run shocks* giving rise to enduring and possibly permanent effects slowly man-

[14] Euro area money market transactions with a three-month maturity observed on the electronic platform e-MID account for less than one percent of the overall trading (Michaud and Upper, 2008). For a study using the e-MID data see Angelini P., Nobili A., and M. C. Picillo (2009) "The Interbank Market After August 2007: What Has Changed and Why?" Banca d'Italia, Temi di Discussione no 731.

[15] There are different types of liquidity risk. From the perspective of this study identifying them is not relevant, but it is gauging the overall effect produced by the ECB's measures in restoring the liquidity levels, and thus the ease of trade, for the normal functioning of the money market in the euro area.

ifesting themselves; 2) *medium-run shocks* giving rise to transitory effects manifesting themselves faster than the long-run shocks; 3) *short-run shocks* giving rise to quickly visible, but short-lived effects. In turn, these otherwise unidentified forces, which act on $z(t)$ simultaneously, govern the evolution, respectively, of the low-, medium- and high-frequency components of the time series. The procedure ensures that three frequency components are essentially orthogonal to each other, and that their sum reproduces the original series $z(t)$ with a negligible frequency decomposition error. The thesis of this paper is that the shocks explaining the evolution of the monetary and liquidity policy measures and the counterparty credit risk concerns as measured by the *iTraxxFS*, have at the same time steered the Euribor-Eurepo spread.

We explicitly model the evolution of each frequency component of $z(t)$ with an independent, parsimonious, state-space model. Hence, the models of the frequency components additively decompose the time series. In this case, the frequency decomposition is viewed as a method for modeling and estimating a variable, for decomposing it into frequencies, and for forecasting its behavior (Watson, 1986).

As originally advocated by Harvey (1985), we extract the frequency components (and the shocks driving them) by smoothing and the estimation of the parameters of the state-space models is carried out in the time domain. In particular, to perform the frequency decomposition we employ three low, band-pass filters, which through their recursions ensure that each frequency component evolves within its pre-specified frequency bandwidth correcting at the same time for possible model misspecifications and approximations in addition to data measurement errors.

The choice of this frequency decomposition approach is motivated by the fact that: 1) it allows us to investigate the behavior of the frequency components in the frequency domain by working in the more familiar time domain; 2) it permits to decompose also nonstationary time series; 3) it uses all of the available data points of $z(t)$; 4) and, importantly, that the frequency decomposition is carried out in *real time*, which means that the decomposition at time t is performed without requiring the knowledge of the values which the series will take on at time $t+1$, and without altering the outcomes of the decomposition already performed at time $t-1$. This is a useful property for a study investigating how monetary policy has progressively influenced money market interest rates.

In what follows we describe how we apply this approach to our study.

4.1 From the Time Domain to the Frequency Domain

Following the procedure proposed by Donati (1971), we simultaneously decompose with finite resolutions the power of $z(t)$ both in the frequency domain and in the time domain. We associate to the frequency range in which $z(t)$ is defined, that is $[0 \div f_{max}]$ where $f_{max} = \frac{1}{2T}$ and T equals one day, four finite frequency resolution intervals: a low-frequency domain $[0 \div f_{lf}]$, a medium-frequency domain $[f_{lf} \div f_{mf}]$, a high-frequency domain $[f_{mf} \div f_{hf}]$ and a residual frequency domain $[f_{hf} \div f_{max}]$.

Then, we associate to each of these frequency domains four finite time resolution intervals T_{lf}, T_{mf}, T_{hf} and T_{max}, respectively, selected in such a way that the product of the frequency and the time intervals is strictly greater than one: $T_{lf} \cdot f_{lf} \gg 1$, $[T_{mf} \cdot (f_{mf} - f_{lf})] \gg 1, [T_{hf} \cdot (f_{hf} - f_{mf})] \gg 1$ and $[T_{max} \cdot (f_{max} - f_{hf})] \gg 1$. By "locally averaging" over the time resolution intervals T_{lf}, T_{mf}, T_{hf} and T_{max} the power of $z(t)$ we partition it into a *low-frequency component* $z_{lf}(t)$, a *medium-frequency component* $z_{mf}(t)$, a *high-frequency component* $z_{hf}(t)$, and a residual frequency component $we(t)$,

$$z(t) = z_{lf}(t) + z_{mf}(t) + z_{hf}(t) + we(t) \tag{1}$$

in such a way that with a reasonable approximation the "locally averaged" power of the four frequency components corresponds to the partitions into the four frequency domains $[0 \div f_{lf}]$, $[f_{lf} \div f_{mf}]$, $[f_{mf} \div f_{hf}]$ and $[f_{hf} \div f_{fmax}]$ (see Appendix I for details). When time resolution intervals larger than T_{lf}, T_{mf}, T_{hf} and T_{max} are considered, the four frequency components of $z(t)$ are orthogonal to each other. As a result, each frequency component of $z(t)$ can be considered independently both when processing the data and when assessing the results. The residual frequency component, $we(t)$, being essentially noise from the viewpoint of this study will not be examined.

4.2 The Dynamic Model of the Frequency Components

We model the behavior of the low-, medium-, and high-frequency component $z_{lf}(t)$, $z_{mf}(t)$ and $z_{hf}(t)$ in which we decompose the time series $z(t)$ with three linear, parameter time-invariant, single-input single-output (SISO), $2^{nd}-$ order (i.e. working with two state variables) dynamic systems, denoted M_{lf}, M_{mf}, and M_{hf}, which have the following specification:

$$\begin{bmatrix} q_{j,1}(t+1) \\ q_{j,2}(t+1) \end{bmatrix} = \begin{bmatrix} 1 - a_j & -b_j \\ 1 & 1 \end{bmatrix} \begin{bmatrix} q_{j,1}(t) \\ q_{j,2}(t) \end{bmatrix} + \begin{bmatrix} 1 \\ 0 \end{bmatrix} u_j(t) \tag{2}$$

$$z_j(t+1) = q_{j,2}(t+1) \qquad j = lf,\, mf,\, hf \tag{3}$$

in which eq. (2) is the state transition equation and eq. (3) is the output, or observation, equation. In the state equation, the (2×1) vector $\mathbf{q}_j(t)$ is the state vector, $u_j(t)$ is the single input, or shock, or exogenous force, steering the dynamics of the system, and $(a_j,\ b_j)$ are real, time-invariant, parameters that are in one-to-one correspondence with the eigenvalues of the state transition matrix of the system, and which will be optimally identified within the frequency bandwidth of interest by minimizing the out-of-sample prediction errors of $z(t)$, as explained next. In the output equation, the frequency component $z_j(t+1)$ takes on the value of the state variable $q_{j,2}(t+1)$.

Notice that the model includes no disturbances in the observation equation. This means that the system output $z_j(t)$, namely the value taken on at time t by the frequency component j, is

driven solely by the single input $u_j(k)$ for $k = t-1, t-2, \ldots, 0$ that acted upon the system M_j before time t. This also means that, by construction, the *effects* which are observed in the behavior of the frequency components follow in time the *causes,* i.e. the system inputs, affecting $z(t)$.

4.3 The Model of the Low Band-Pass Filter

The inputs $u_{lf}(t)$, $u_{mf}(t)$ and $u_{hf}(t)$ of eq. (2) steering the dynamics of the frequency components of the time series $z(t)$ are unknown and need to be estimated. Also the six state variables $\mathbf{q}_{lf}(t)$, $\mathbf{q}_{mf}(t)$ and $\mathbf{q}_{hf}(t)$ of the systems M_{lf}, M_{mf} and M_{hf}, which altogether model the dynamics of $z(t)$, are not directly accessible to measurement and need therefore to be estimated. To compute $u_j(t)$ and to estimate $\mathbf{q}_j(t)$ for *j=lf, mf, hf,* we use three dynamic low-, band-pass filter, namely three input-output state observers, that extract the required information from $z(t)$, by working simultaneously within three pre-defined frequency bandwidths $[0 \div f_{lf}]$, $[f_{lf} \div f_{mf}]$ and $[f_{mf} \div f_{hf}]$. The state observers are themselves linear, time-invariant, dynamic systems with the same functional form as the systems M_j, for *j=lf, mf, hf,* and they act on the systems M_j through closed-loop recursions. The mathematical details of the frequency decomposition are illustrated in Appendix II.

As a result of the reiterations of the filters, at each point in time t the sum of the three frequency components does not significantly differ from the actual value of $z(t)$, i.e. $z_{lf}(t) + z_{mf}(t) + z_{hf}(t) \cong z(t)$. In ensuring such outcome, the dynamic filters also correct for possible misspecifications in the models M_j and for the effects of measurement errors contained in $z(t)$.

We denote M the overall dynamic model of $z(t)$ including the three input-output state observers. Its equations are:

$$\mathbf{q}(t+1) = \mathbf{H}\mathbf{q}(t) + \mathbf{B}z(t) \tag{4}$$

$$\mathbf{y}(t+1) = \mathbf{G}\mathbf{q}(t+1) \tag{5}$$

with state transition eq. (13) the function $z(t)$ is decomposed into three frequency components by means of the (12×1) state vector $\mathbf{q}(t)$ – which includes the six state variables $\mathbf{q}_{lf}(t)$, $\mathbf{q}_{mf}(t)$ and $\mathbf{q}_{hf}(t)$ of the systems M_{lf}, M_{mf}, and M_{hf} and as many state variables used by the filters – the real, time-invariant (12×1) vector of parameters $\mathbf{B}$, and the real, time invariant (12×12) state transition matrix $\mathbf{H}$, which includes the state transition matrices of the systems M_j for *j=lf, mf, hf* and of the filters. With observation eq. (14) the real, time-invariant, (7×12) matrix $\mathbf{G}$ turns the state vector $\mathbf{q}(t+1)$ into the one-step-ahead forecast output vector $\mathbf{y}(t+1)$ with $\mathbf{y} \equiv \begin{bmatrix} u_{lf} & u_{mf} & u_{hf} & z_{lf} & z_{mf} & z_{hf} & \hat{z} \end{bmatrix}$ where $\hat{z}(t+1)$ is the one-step ahead forecast of the function $z(t)$. The matrices $\mathbf{B}$, $\mathbf{H}$, and $\mathbf{G}$ are presented in detail in Appendix II.

To produce out-of-sample forecasts for time horizons $\tau \in [1, h]$, we proceed recursively and use the outputs of the model M, i.e. its one-step-ahead predictions, as its next-step inputs for $\tau - 1$

times.

The advantage of this filtering approach is that it allows us to simultaneously extract the low-, medium-, and high-frequency components of $z(t)$ within the pre-selected frequency intervals $[0 \div f_{lf}]$, $[f_{lf} \div f_{mf}]$ and $[f_{mf} \div f_{hf}]$ without actually having to think in terms of frequency bandwidths, if we do not wish to. The reason is that the selection of the frequency bandwidths is the automatic outcome of the choice we are instead called to make of the eigenvalues (or poles) of the matrix $\mathbf{H}$. As explained in Appendix II, the selection of the 12 values to assign to the 12 poles of $\mathbf{H}$ actually reduces to the selection of three different eigenvalues p, with $p \in (0,1)$, defining the three frequency bandwidths.

Denote T the sampling period of $z(t)$, which in our case is one day ($T = 1$). Then, the value p_j (pure number) for j=*lf, mf, hf*, of the poles used to extract the frequency component $z_j(t)$, is related to the upper bound f_j^{up} of the frequency bandwidth (measured in cycles/day) by the equation: $p_j = e^{-2\pi f_j^{up} T}$. At the same time, f_j^{up} is related to the time constant[16] τ_j for j=*lf, mf, hf*, characterizing the step or impulse response of the filters, by the relation $\tau_j = 1/2\pi f^{up}$. In this study, the time constants of the state observers characterize the persistence of the shocks $u_j(t)$ steering the dynamics of the frequency components. We undertake that when a lapse of time corresponding to one time constant has passed from the inception of the shock $u_j(t)$, the effect produced by that force on the corresponding frequency component $z_j(t)$ has become fully manifest.

As a result, by exogenously setting the eigenvalues of the matrix $\mathbf{H}$ we are able to define both the upper bound of the frequency intervals $[0 \div f_{lf}]$, $[f_{lf} \div f_{mf}]$ and $[f_{mf} \div f_{hf}]$ within which we decompose the function $z(t)$ and the time constants clustering the shocks steering $z(t)$ according to their persistence.

In Table 1 we present the eigenvalues we assign to the matrix $\mathbf{H}$ in this study along with the corresponding frequency bandwidths and values of the time constants. In particular, the *long-run shocks*, which give rise to enduring effects that may persist up to infinity, are extracted from $z(t)$ within the frequency bandwidth of $[0 \div 0.002]$ rad/day. This means that the oscillations with a period longer than 625 days pass,[17] whereas the oscillations with a period significantly lower than that − that are therefore more frequent − do not pass but get filtered by the state observer associated to the system M_{mf}. This also means that we define long-run shocks those shocks whose effect broadly takes at least 99.5 working days (about 5 months) before becoming fully manifest. Through the model M_{lf} of eqs. (2) and (3) from the long-run shocks we obtain the low-frequency component $z_{lf}(t)$.

The *medium-run shocks* are extracted within the frequency range of $[0.002 \div 0.02]$ rad/day

[16] The time constant τ represents the time it takes the response of the state observer to reach about 63 percent of its final asymptotic value.

[17] For $f > f_{lf}^{up}$ frequency values the filter introduces an attenuation, which on account of the fact that all of its four poles take on the same value, is described by the law $g(f) = \left(f/f_{lf}^{up}\right)^{-4} = (1/\sqrt{2} * 1/\sqrt{2} * 1/\sqrt{2} * 1/\sqrt{2}) = 0.25$.

Table 1: The Filter's Eigenvalues and the Frequency Bandwidths

Frequency component	Frequency Domain		Band-Pass Filter	
	Frequency Bandwidth f^{low}, f^{up} (*cycles/day*)	Period $1/f^{up}$ (*days*)	Poles $p = e^{-2\pi f^{up} T}$ (*pure number*)	Time Constant $\tau = 1/2\pi f^{up}$ (*days*)
Low-frequency	$[0 \div 0.002]$	$T > 625$	0.99	99.5
Medium-frequency	$[0.002 \div 0.02]$	$49 < T < 625$	0.88	$7.8 < \tau < 99.5$
High- frequency	$[0.02 \div 0.06]$	$17.6 < T < 49$	0.70	$2.8 < \tau < 7.8$

This table reports the eigenvalues assigned to the matrix **H** to perform the frequency decomposition of the time series $z(t)$, the corresponding frequency bandwidths in which we extract the three frequency components of $z(t)$, and the period of the corresponding cycles. In the time domain, these are related to the persistence of the shocks u_{lf}, u_{mf}, and u_{hf} steering the dynamics of $z(t)$, which we also extract. The time constants reported in the table represent the time it takes for the effect produced by such shocks on the frequency components to become fully manifest.

from the time series obtained after removing the low-frequency component from $z(t)$. The medium-frequency component is then characterized by a period of at least 49 working days, but significantly lower than 625 days. Equivalently, the effect of the medium-run shocks broadly take at least 7.8 working days, but less than 99.5 working days, to become fully manifest.

The *short-run shocks*, are extracted within the frequency bandwidth of $[0.02 \div 0.06]$ rad/day from the time series obtained after removing the low- and medium-frequency components from $z(t)$. The high-frequency component is then characterized by a period of at least 17.6 working days, but significantly lower than 49 working days. Equivalently, the effects of the short-lived shocks broadly take at least 2.8 working days, but less than 7.8 working days, to become fully manifest.

The residual time series obtained after removing the low-, medium-, and high-frequency components from $z(t)$, which lies in the residual frequency range $[0.06 \div 3.14]$ rad/day, is neglected here because it is too noisy and little informative for the purpose of this study.

4.4 Parameter Estimation Procedure

In order to enhance the robustness of the model, the parameters $(a_j,\ b_j)$ of the systems M_j, for *j=lf, mf, hf*, are not identified in sample, but on the out-of-sample forecasts of $z(t)$, with the exception of the parameter b_{lf} which is *a priori* imposed to be zero for the effect produced by the long-run shocks to possibly persist up to infinity. The remaining parameters are estimated jointly by minimizing

the following quadratic loss functional Ft :

$$\min_{a_j, b_p} Ft = \sum_{t=t_1}^{t_2-1} \sum_{\tau=1}^{100} [fe(t,\tau)w(\tau)]^2 \qquad j = lf,\, mf,\, hf \qquad p = mf,\, hf \tag{6}$$

where $fe(t,\tau) = z(t+\tau) - \hat{z}(t+\tau)$ for $\tau = 1, \ldots, 100$ days, are the out-of-sample forecast errors of $z(t)$, and $w(\tau) = \exp(-\tau/500)$ is a negative exponential function attaching to the forecast errors a weight slightly decreasing with the lengthening of the prediction horizon τ, while t_1, t_2 are, respectively, the beginning and the end of the data sample selected to identify the parameters. Notice that the length of such samples should meet the constraints discussed in section 4.1. In particular, on account of the frequency intervals presented in Table 1, in this study it should be that $T_{lf} \gg 500$ days, $T_{mf} \gg 56$ days, and $T_{hf} \gg 25$ days. Yet, given that the *LTRO6m* were introduced in April 2008, the *STRO* were introduced in September 2008, and the *LTRO1Y* in June 2009, and this study ends on 30 November 2009, the constraint on the time resolution interval T_{lf} for these liquidity measures cannot be met, which may make it difficult to fully disentangle the low- from the medium-frequency components of these variables. Given the limited number of observations for *LTRO1Y* we add this variable to the *LTRO6m*, giving rise to the very long-term refinancing operations denoted *LTRO6m1Y*. We set $t_1 =$ 3 October 2005. After testing different sub-samples we obtain that the parameters for the *MPR*, the *MRO* and *LTRO3m* remain essentially unchanged after end December 2008. Instead, the parameter values for the remaining variables, if re-estimated every couple of months, keep on varying, albeit by very little (the changes are of the order of 0.01% to 0.1%). The estimates presented in Table 2 refer to $t_2 =$ 30 November 2009.

To minimize the functional Ft we employ the numerical algorithm based on the conjugate-gradient method contained in the software suite EicasLab whose embedded tests check for the local uniqueness of the minimum.

5 Results of the Univariate Frequency Decomposition

The outputs of the univariate frequency decomposition model M of eqs.(13) and (14) include the one-step-ahead forecasts of the time series $z(t)$ being decomposed, obtained as the sum of the predictions of its low-, medium-, and high-frequency components. Then, first, to evaluate the performance of the model M, we compute the root mean square error of the prediction errors of $z(t)$, i.e. $RMSE = \sqrt{\frac{1}{1086}\sum_{t=1}^{1086} fe(t,1)}$. Given that the variables being decomposed are expressed in different units of measure, to allow for comparisons, we divide the $RMSE$ by the root mean square value of their time series $z(t)$, $RMSV = \sqrt{\frac{1}{1086}\sum_{t=1}^{1086} z(t)}$. The $RMSE/RMSV$ ratios reported in Table 3 are all very small and close to zero, which indicates that the estimated models M explain (and predict) the series satisfactorily. Moreover, given that the autocorrelation of the forecast errors

Table 2: Parameter Values of the Univariate Frequency Decomposition Models

Variable	LF		MF		HF	
	Parameter		Parameter		Parameter	
	a	*b*	*a*	*b*	*a*	*b*
Spread	4.781E-03	0.000E+00	3.852E-01	4.240E-04	3.061E-01	8.107E-02
MPR	3.824E-03	0.000E+00	2.664E-01	1.023E-03	3.460E-01	4.490E-02
MRO	4.829E-03	0.000E+00	3.899E-02	7.841E-04	2.518E-01	1.053E-01
STRO	5.906E-03	0.000E+00	2.405E-01	3.278E-03	7.216E-02	1.332E-02
LTRO3m	1.073E-03	0.000E+00	2.090E-02	6.457E-04	3.984E-01	8.349E-02
LTRO6m	2.521E-03	0.000E+00	2.813E-02	3.271E-04	3.147E-01	1.028E-01
LTRO6m1Y	0.000E+00	0.000E+00	2.761E-02	4.240E-04	3.061E-01	8.107E-02
iTraxxSF	4.595E-03	0.000E+00	3.649E-01	9.968E-03	2.709E-01	1.875E-02

This table reports the estimates of the parameters of the univariate decomposition models M_{lf}, M_{mf}, and M_{hf}, used to decompose the time series of the $Spread$, MPR, MRO, $STRO$, $LTRO3m$, $LTRO6m$, $LTRO6m1Y$, and the $iTraxxFS$ into a low-frequency component (LF), a medium-frequency component (MF), and a high-frequency component (HF) and to extract the long-, medium-, and short-run shocks driving their evolution over the period 3 October 2005 to 30 November 2009.

$fe(t,1)$ at displacements of one day and one week are close to zero, the forecast errors $fe(t,1)$ are due to innovations, and as such that they are unpredictable. The model M performs worse than the average in decomposing (and predicting) the $STRO$ due to the relatively few observations available for this variable, as remarked in section 4.4.

Second, we compute the pairwise correlations between the frequency components extracted from each series. On account of the short length of the series, as a rule of thumb we consider the correlation to be significant if bigger than $|0.25|$. The results reported in Table 3 show that the correlation between the low-frequency component (LF) and the medium-frequent component (MF) for all series remain below the benchmark, excepted for the $LTRO6m1Y$. The correlation between the MF and the high-frequency component (HF) stays for all series close to zero, again with the exception of the $LTRO6m1Y$. The model M performs worse than average in decomposing the $LTRO6m1Y$ because this is a rather short series. However, notice that even though there are too few observations for the dynamic filter to accurately separate out the trends from the cycles of this variable, no information goes lost. In fact, the advantage of this filtering approach is that it permits us to extract from the data more than one frequency component at the same time minimizing the information loss when switching from a frequency bandwidth to the other, because the decomposition procedure ensures that the sum of the three frequency components reconstructs the actual pattern of $z(t)$. As a result, the oscillations whose period is neither significantly lower nor significantly higher than the selected frequency cuts end up with being captured by one of two neighboring frequency domains. The frequency components extracted from the variables are plotted

Table 3: Summary Statistics: The Frequency Decomposition of the Variables

Variables	RMSE / RMSV	Autocorrelations of $fe(t,1)$		Pairwise Correlations	
		Lag (1D)	Lag (1W)	LF and MF	MF and HF
Spread	0.03	-0.04	-0.09	-0.10	0.04
MPR	0.01	0.01	0.00	0.11	0.07
MRO	0.06	0.02	0.03	0.20	-0.04
STRO	0.16	0.48	-0.09	0.06	0.09
LTRO3m	0.02	-0.01	0.00	-0.13	0.07
LTRO6m	0.04	0.04	0.04	-0.18	0.07
LTRO6m1Y	0.07	0.01	0.02	0.44	-0.13
iTraxxSF	0.08	-0.02	-0.08	-0.08	-0.01

This table reports the ratio between the root mean square error (RMSE) of the one-step ahead predictions of the variables, and the root mean square value (RMSV) of the variables, and the autocorrelation of the forecast errors at displacements of 1 day and 1 week. The last two columns show the pairwise correlations between the low-frequency component (LF) and the medium-frequency component (MF), and between the MF and the high-frequency component (HF) extracted from the series. The daily data used in the estimation cover the period from 3 October 2005 to 30 November 2009.

in Figure 1 and Figure 2.

Finally, for the considered financial variables to cause a change in the Euribor-Eurepo spread, the shocks explaining their evolution and the shocks extracted from the *Spread* should be uncorrelated. In fact, given that the cause always comes before the effect, no matter how small the time elapsing between the two, for one variable to cause a change in another variable, the existence of a contemporaneous relationship between the two should be excluded. Therefore, we compute the pairwise correlations among the estimated shocks $\hat{u}^i_j(t)$, for $i = MPR$, MRO, $STRO$, $LTRO3m$, $LTRO6m1Y$, *iTraxxFS,* and *j=lf, mf, hf*, and the inputs $\hat{u}^o_j(t)$ extracted from the *Spread*. The results presented in Tables 4 show that there is no significant (contemporaneous) correlation between the changes in the ECB's monetary and liquidity measures, the changes in *iTraxxFS* and the changes in the money market spreads. These results support the potential explanatory power of the investigated financial variables for the *Spread*. This issue is addressed in the next section.

6 The Multivariate Frequency Decomposition Model

In this section we extend the univariate approach introduced by Donati and Donati (2008) to the multivariate framework. Specifically, we propose a procedure to decompose in *real time*, in frequency components lying within pre-specified frequency bandwidths, the variable $z^o(t)$ denoted the *dependent* variable, evaluating at the same time if and in what measure the long-, medium- and short-run shocks governing the evolution of a set of *independent* variables $z^i(t)$ for $i = 1, , \ldots, n$

Figure 1: The Frequency Components of the Variables

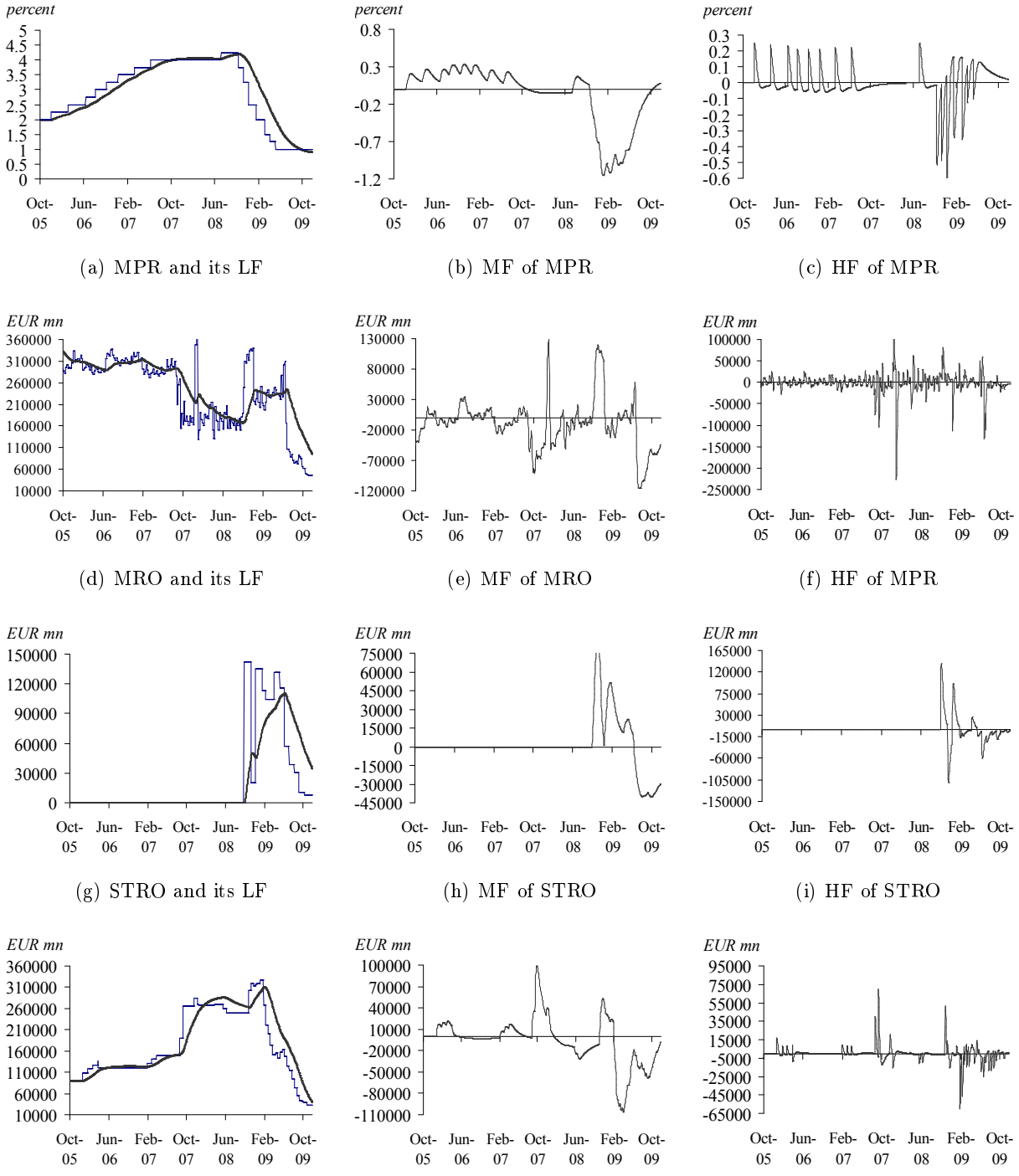

(a) MPR and its LF (b) MF of MPR (c) HF of MPR

(d) MRO and its LF (e) MF of MRO (f) HF of MPR

(g) STRO and its LF (h) MF of STRO (i) HF of STRO

(j) LTRO3m and its LF (k) MF of LTRO3m (l) HF of LTRO3m

The graphs on the left-hand side show the monetary policy rate MPR, the main refinancing operations MRO, the special-term refinancing operations $STRO$ and the refinancing operations with three-month maturity $LTRO3m$ together with their low-frequency components (LF). The graphs in the center and on the right-hand side show the medium-frequency components (MF) and high-frequency components (HF) of the same variables. The considered period goes from 3 October 2005 to 30 November 2009.

Figure 2: The Frequency Components of the Variables

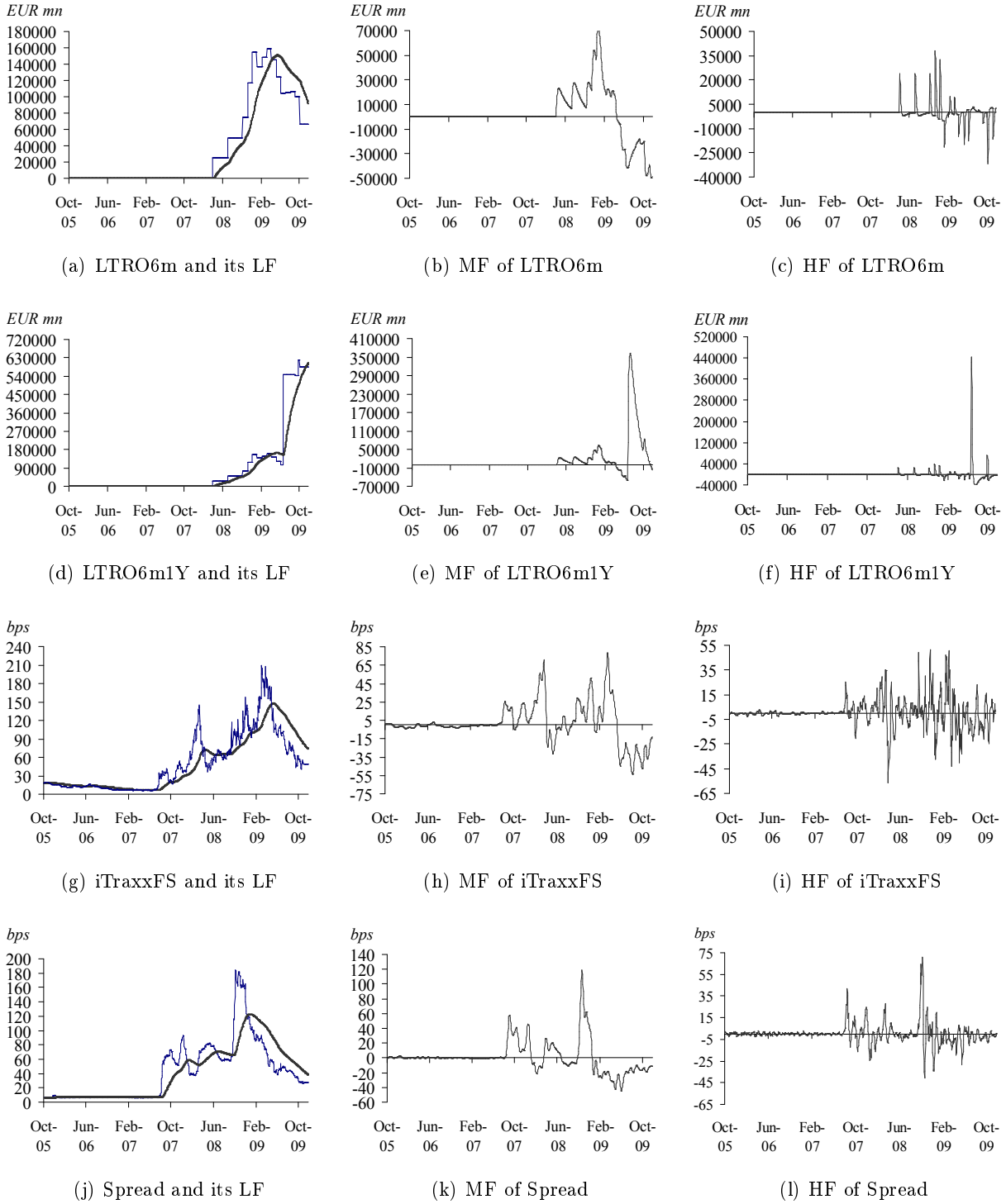

(a) LTRO6m and its LF (b) MF of LTRO6m (c) HF of LTRO6m

(d) LTRO6m1Y and its LF (e) MF of LTRO6m1Y (f) HF of LTRO6m1Y

(g) iTraxxFS and its LF (h) MF of iTraxxFS (i) HF of iTraxxFS

(j) Spread and its LF (k) MF of Spread (l) HF of Spread

The graphs on the left-hand side show the refinancing operations with six-month maturity $LTRO6m$, and with six- and one-year maturity $LTRO6m1Y$, the iTraxx financial senior index $iTraxxFS$, and the $Spread$ between the Euribor and the Eurepo with three-month maturity, together with their low-frequency components (LF). The graphs in the center and on the right-hand side show the medium-frequency components (MF) and high-frequency components (HF) of the same series. The considered period goes from 3 October 2005 to 30 November 2009.

Table 4: Pairwise Correlations Between Long-, Medium-, and Short-Run Shocks

Pairwise Correlations Between the Long-Run Shocks Steering the Low-Frequency Components								
	Spread	*MPR*	*MRO*	*STRO*	*LTRO3m*	*LTRO6m*	*LTRO6m1Y*	*iTraxxFS*
Spread	1							
MPR	0.20	1						
MRO	0.16	0.06	1					
STRO	0.21	-0.02	-0.15	1				
LTRO3m	0.04	-0.04	-0.02	0.00	1			
LTRO6m	0.02	-0.26	-0.11	0.04	-0.03	1		
LTRO6m1Y	0.04	-0.02	-0.33	0.02	-0.11	0.20	1	
iTraxxFS	0.05	-0.01	0.03	-0.04	-0.18	-0.01	0.00	1

Pairwise Correlations Between the Medium-Run Shocks Steering the Medium-Frequency Components								
	Spread	*MPR*	*MRO*	*STRO*	*LTRO3m*	*LTRO6m*	*LTRO6m1Y*	*iTraxxFS*
Spread	1							
MPR	0.12	1						
MRO	0.06	0.02	1					
STRO	0.22	-0.18	0.02	1				
LTRO3m	-0.04	0.02	0.04	0.05	1			
LTRO6m	0.02	-0.03	-0.06	0.00	0.00	1		
LTRO6m1Y	0.01	0.00	-0.13	-0.02	-0.14	0.21	1	
iTraxxFS	0.02	-0.04	-0.01	-0.10	0.06	-0.02	0.04	1

Pairwise Correlations Between the Short-Run Shocks Steering the High-Frequency Components								
	Spread	*MPR*	*MRO*	*STRO*	*LTRO3m*	*LTRO6m*	*LTRO6m1Y*	*iTraxxFS*
Spread	1							
MPR	0.00	1						
MRO	-0.02	0.08	1					
STRO	-0.01	0.16	-0.04	1				
LTRO3m	0.03	-0.01	0.00	0.03	1			
LTRO6m	0.00	0.00	0.00	0.08	0.01	1		
LTRO6m1Y	0.10	0.01	0.01	0.01	-0.14	0.19	1	
iTraxxFS	0.09	-0.04	-0.02	-0.01	-0.07	-0.04	0.03	1

These tables report the pairwise correlations between the long-, medium-, and short-run shocks $\hat{u}^i_{lf}(t)$, $\hat{u}^i_{mf}(t)$ and $\hat{u}^i_{hf}(t)$ driving, respectively, the LF, MF, and HF of the monetary policy rate MPR, the main refinancing operations MRO, the special-term refinancing operations $STRO$, the long-term refinancing operations with three-month and six-month maturity $LTRO3m$ and $LTRO6m$, and the refinancing operations with six- and one-year maturity $LTRO6m1Y$, the iTraxx financial senior index $iTraxxFS$, and the long-, medium-, and short-run shocks $\hat{u}^o_{lf}(t)$, $\hat{u}^o_{mf}(t)$ and $\hat{u}^o_{hf}(t)$ driving the LF, MF, and HF of the Euribor-Eurepo spreads with 3-month maturity, $Spread$. The daily data used in the estimation cover the period from 3 October 2005 to 30 November 2009.

contribute to drive also $z^o(t)$.

Following the procedure illustrated in section 4, we decompose into three frequency components each independent variable $z^i(t)$ obtaining as a result the long-, medium- and short-run inputs $u^i_{lf}(t)$, $u^i_{mf}(t)$ and $u^i_{hf}(t)$ for $i = 1, , \ldots, n$ steering their dynamics. We presume that these shocks contribute, in conjunction with a number of other unidentified forces denoted $u^o_j(t)$, for *j=lf, mf, hf*, to drive the frequency components $z^o_j(t)$, for *j=lf, mf, hf*, of the dependent variable $z^o(t)$. We denote $z^{o,i}_j(t)$ the effect produced on the frequency component $z^o_j(t)$ by the input $u^i_j(t)$, and we denote $z^{o,o}_j(t)$ the effect produced by the input $u^o_j(t)$. Thus, $z^o_j(t) = z^{o,o}_j(t) + \sum_{i=1}^{n} z^{o,i}_j(t)$. The total effect produced by each independent variable $m = i, o$ on the dependent variable is then denoted:

$$z^{o,m}(t) = z^{o,m}_{lf}(t) + z^{o,m}_{mf}(t) + z^{o,m}_{hf}(t) \tag{7}$$

The model M^o explaining the dynamics of the frequency components of $z^o(t)$ is then a multiple-input multiple-output (MIMO) dynamic system composed of $(n + 1)$ single-input single-output (SISO) systems modeling the relationship between the inputs $u^i_j(t)$ and $u^o_j(t)$ and the frequency component shares $z^{o,i}_j(t)$ and $z^{o,o}_j(t)$, respectively. In order to allow for the possibility that the relationships with the independent variables changes with time, these SISO systems, denoted $M^{o,m}_j$ for $m = i, o$ and $i = 1, \ldots, n$, are linear, time-variant, dynamic system having the following specification:

$$\begin{bmatrix} q^{o,m}_{j,1}(t+1) \\ q^{o,m}_{j,2}(t+1) \end{bmatrix} = \begin{bmatrix} 1 - a^{o,m}_j(t) & -b^{o,m}_j(t) \\ 1 & 1 \end{bmatrix} \begin{bmatrix} q^{o,m}_{j,1}(t) \\ q^{o,m}_{j,2}(t) \end{bmatrix} + \begin{bmatrix} 1 \\ 0 \end{bmatrix} u^m_j(t) \tag{8}$$

$$z^{o,m}_j(t) \quad = \alpha^{o,m}_j(t) q^{o,m}_{j,2}(t) \qquad\qquad m = i, o \qquad j = lf, mf, hf \tag{9}$$

where state eq. (8) consists of a (2×1) vector of state variables $\mathbf{q}^{o,m}_j(t)$, a state transition matrix characterized by the real, time-variant parameters $\left(a^{o,m}_j(t),\ b^{o,m}_j(t)\right)$, and the input $u^m_j(t)$, whose contribution $z^{o,m}_j(t)$ to the dynamics of the frequency component $z^o_j(t)$ is gauged by the real, time-variant, parameter $\alpha^{o,m}_j(t)$, as shown in output eq. (9).

We presume that each generic time-dependent parameter, generically denoted $k(t)$, evolves according to the following laws:

$$\begin{aligned} k(t) &= k_a + k_o \exp\left(\tfrac{t - Ts}{T_c}\right) \qquad \text{if} \quad t < Ts \\ k(t) &= k_b - k_o \exp\left(\tfrac{Ts - t}{T_c}\right) \qquad \text{if} \quad t > Ts \end{aligned} \tag{10}$$

with

$$k_o = \frac{k_b - k_a}{2} \tag{11}$$

where k_a is the value taken on by $k(t)$ for $t \rightarrow -\infty$ and k_b is the value it takes on for $t \rightarrow +\infty$; moreover, Ts is the data point at the center of the transition from k_a to k_b; finally, Tc is the time constant characterizing the decay of the exponential law linking k_a to k_b. To simplify notation denote this group of parameters $k_j^{o,m} = \left(\begin{array}{cccc} k_{j,a}^{o,m}, & k_{j,b}^{o,m}, & Ts_j^{o,m}, & Tc_j^{o,m} \end{array} \right)$ for $m = i, o$ and j=*lf, mf, hf*.

To estimate the latent state variables of the model M^o we use three dynamic filters and we follow the procedure described in section 4.3; therefore, when we refer to the model M^o we refer to the model composed of eqs.(8), (9), (10), (11) and of the three input-out state observes described in Appendix II. To identify the time-variant parameters of M^o we minimize the quadratic loss functional Fu defined on the out-of-sample forecast errors $fe^o(t,\tau) = z^o(t+\tau) - \hat{z^o}(t+\tau)$, of the dependent variable $z^o(t)$, for $\tau = 1, \ldots, 100$ days,

$$\min_{k_j^{o,m}, a_j^{o,m}, b_p^{o,m}, \alpha_j^{o,m}} Fu = \sum_{t=t_1}^{t_2-1} \sum_{\tau=1}^{100} [fe^o(t,\tau) w(\tau)]^2 \qquad j = lf,\, mf,\, hf \qquad m = i, o \qquad p = mf,\, hf \tag{12}$$

where t_1, t_2 are, respectively, the beginning and the end of the employed data sample, and $w(\tau) = \exp(-\tau/50)$ is a negative exponential function introduced to avoid that the forecast errors matter in the same way for the identification of the parameter values, independently of the forecast horizon they refer to. Specifically, this function attaches full importance (i.e. a weight of 100%) to the one-day ahead forecast errors, and gradually less importance to the errors made for longer prediction horizons: for example, the errors made in predicting the dependent variable 50 days beforehand have a weight of 36%, while the 100−day ahead forecast errors have a weight of only 14%.

We minimize Fu using the numerical algorithm based on the conjugate-gradient method contained in the software suite EicasLab whose embedded tests check for the local uniqueness of the minimum. The parameters of the model M^o are estimated together with their standard deviations.

7 Results: The Effect of the ECB's Measures

To evaluate the effect produced by the ECB's monetary and liquidity policies and by the market participants' credit risk concerns as measured by the iTraxx financial senior index, *iTraxxFS,* over the period 3 October 2005 - 30 November 2009, we estimate the model M^o described in section 6 in which the dependent variable is the Euribor-Eurepo spread with 3-month maturity (*Spread*).

7.1 Model Validation Analysis

To assess if the model M^o serves the purpose, given its output are the predictions of the *Spread*, first we contrast its performance with a benchmark model, namely the random walk model. The best

Table 5: Summary Statistics: The Money Market Spread Fitting Errors

Mean	Std. Dev.	Max	Min	RMSE	Autocorrelations		
(*basis points*)	(*basis points*)	(*basis points*)	(*basis points*)	(*basis points*)	Lag (1D)	Lag (1W)	Lag (1M)
0.28	4.69	17.92	-31.98	4.69	0.27	-0.01	0.00

This table reports the mean, the standard deviation, the maximum and the minimum of the one-step-ahead forecast errors $fe(t,1)= Spread(t,1) - \hat{Spread}(t,1)$ where $\hat{Spread}(t,1)$ are the output of the model M^o over the period 1 August 2007 - 30 November 2009. The fifth column of the table reports the root mean square error of the $fe(t,1)$. The last three columns show the autocorrelation of the forecast errors at displacements of 1 day, 1 week, and 1 month.

forecast that can be made with the random walk is to predict that tomorrow's value of the *Spread* is equal to today's, because the input of the random walk model is an unpredictable zero-mean white noise. Moreover, given that today's state of the random walk model stems from the sum of purely random, white, inputs, past developments are of no help in forecasting the future behavior of the *Spread* when this model is employed.

Ideally, for the evaluation of the performance of a dynamic model no more inputs (or shocks) should affect the variable being modeled after the beginning of the test. In such case, the outputs of the model (its forecasts) could be directly contrasted with the actual evolution of the series it aims at explaining, and any difference between the two would be ascribed to some model deficiency. However, in general, it is not possible to suspend the flow of shocks driving the series of interest. Hence, it becomes difficult to ascertain whether the prediction errors made by the model are due to model imperfections, or if they are due to the effect of unknown shocks (innovations) that acted after the beginning of the forecast exercise. When besides the identification of the model parameters one estimates also the past inputs that steered the dynamics of the variable of interest as in this study, the following criteria could be used to validate the model: 1) the one-step ahead forecast errors of the model are unpredictable; 2) the adopted model largely outperforms the random walk model in predicting[18] the variable of interest; 3) in spite of the innovations, the model fits (or predicts) the variable of interest, in our case the *Spread*, with acceptable accuracy.

If we use all the information available in our data set and we identify the parameters of model M^o by minimizing the functional Fu of eq. (12) setting t_1 =3 October 2005 and t_2 =30 November 2009, we obtain that the one-step-ahead predictions of the *Spread* over the financial turmoil period, 1 August 2007 - 30 November 2009, have a root mean square error $RMSE = \sqrt{\frac{1}{609}\sum_{t=1}^{609}\left[fe(t,1)\right]^2} =$ 4.69 basis points. As shown in Table 5, the one-step-ahead forecast errors have a mean value of 0.28

[18]Notice that the contrast with the performance of the random walk model is acceptable and relevant for the purpose of model validation both when the predictions are carried out "purely" out of sample, i.e. without updating the model parameters during the forecast exercise, and when all the information available in the data set is first used to identify the model parameters, and the predictive ability of the model is compared with that of the random walk model's thereafter (see A. Inoue and L. Kilian (2004) "In-Sample or Out-of-Sample Tests of Predictability: Which One Should We Use?" Econometric Reviews, 23(4), 371-402).

Figure 3: The Out-of-Sample Forecasts of the Spread

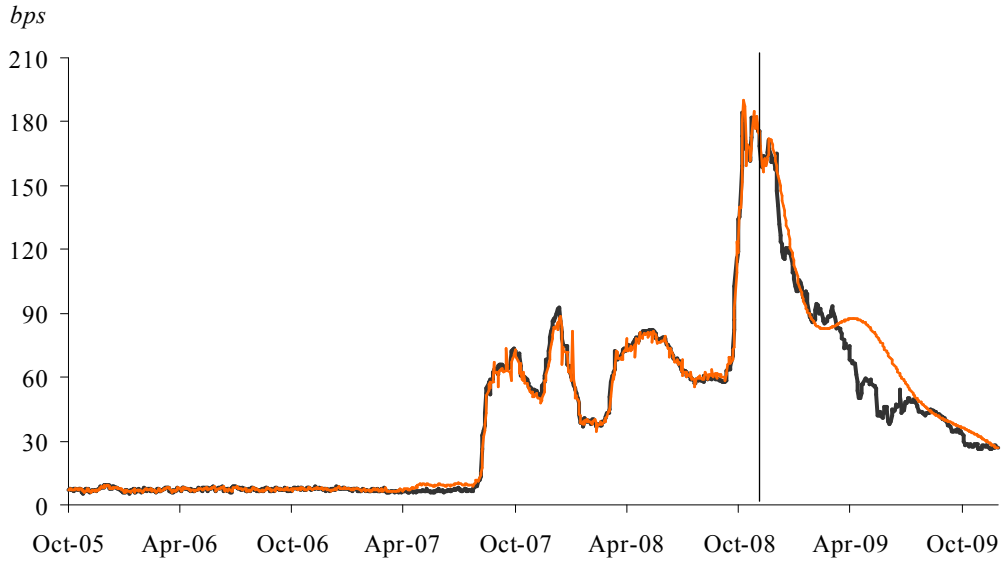

This graph contrasts the actual evolution of the Euribor-Eurepo spread with a 3-month maturity (dark line) with its out-of-sample forecasts performed with the model M^o from 18 November 2008 (signalled by the vertical line) to the end of the sample on 30 November 2009.

basis points, which is close to zero thereby indicating that the predictions are not affected by any systematic bias. Moreover, given that that their autocorrelation at displacements beyond one day is virtually zero, these errors are also unpredictable suggesting that they are due to innovations. Taken together these results satisfy the first condition for the validation of the model M^o.

Next, if we consider the entire data sample, 3 October 2005 to 30 November 2009, we obtain that the random walk model predicts the *Spread* 100−days ahead with a weighted root mean square error of 25.12 basis points, whereas the model M^o predicts the *Spread* over the same forecast horizon with a root mean square error (weighted by the negative exponential function) 2.243 times smaller, of 11.20 basis points. Thus, also the second condition for model validation is satisfied. The better performance of the model M^o is due to the fact that it employs the information provided by past shocks to predict the future behavior of the *Spread*, which helps reduce uncertainty by 55% compared with the complete uncertainty one faces when forecasting with the random walk model. This also means that over 100−day time horizons, 45% of the changes in the *Spread*, compared with the *Spread*'s initial level, are due to unpredictable developments which corroborates the presumption of Caballero and Krishnamurthy (2008) on the major role played by uncertainty in the observed rise of unsecured money market rates.

Finally, we use only part of the data to estimate the model M^o and then check how the model out-of-sample forecasts the *Spread* over the remaining observations. The period we employ to identify the model begins on 3 October 2005 and ends on 18 November 2008, about a month after the ECB

adopted the fixed rate tender procedure with full allotment at the monetary policy rate, it expanded the list of assets eligible as collateral at its refinancing operations, it began reducing the monetary policy rate level, and the EU governments announced a number of fiscal measures in support of their banking systems. We set all inputs $\hat{u}_j^m(t) = 0$, $m = i, o$, *j=lf, mf, hf* of eq. (8) that affected the dynamics of the *Spread* after 18 November 2008 equal to zero and, without further updating the identification of the parameters of the model M^o, we proceed recursively using the outputs of the model M^o, i.e. its one-step-ahead predictions, as its next-step inputs until 30 November 2009. This is equivalent to the case in which, from 18 November 2008 onwards, no further changes occurred to the ECB's measures (i.e. the *MPR* and the outstanding liquidity remained volumes unchanged at the levels where they stood on 18 November 2008), and the *iTraxxFS* and the residual unexplained factors also remained unchanged at their 18 November 2008's levels. As shown in Figure 3, the evolution of these out-of-sample forecasts is close to the actual developments of the *Spread* from mid-November 2008 until mid-March 2009, about when market participants began expecting that the ECB would introduce additional measures to support the normalization of the euro area money market and the transmission mechanism of monetary policy. Such measures were subsequently announced at the ECB press conference of 2 April 2009, and on 7 May 2009 the ECB informed that in the course of 2009 three LTRO with a one-year maturity would be carried out. The difference between the forecasted *Spread* and its actual evolution during the period going from mid-March 2009 to mid-July 2009 can be explained, among other things, with market expectations of, and the actual effect produced by, the ECB's supplementary measures. On 24 June 2009, the first *LTRO1Y* reported the highest ever number of participants (1,121 bidders) and the highest amount ever of liquidity allotted (442 billions EUR) at an ECB refinancing operation. From mid-July 2009 onwards the forecasts resume predicting the *Spread* fairly accurately. These results suggest that the *new* actions carried out by the ECB between end-November 2008 and end-November 2009 have contributed to fully neutralize the effect of any other force pushing the *Spread* upwards.

Altogether, the results presented in this section validate the employment of the model M^o.

7.2 The Pre-Turmoil Period

In this section, we investigate the response of the *Spread* to the ECB's monetary and liquidity policy measures and to the changes in the *iTraxxFS* in the pre-turmoil period going from 3 October 2005 to 28 February 2007 (368 observations).

According to eq. (7), the response $z^{o,i}(t)$ of the *Spread* to each of the i =*MPR*, *MRO*, *LTRO3m*, *iTraxxFS* considered independent variables is composed by the sum of its response $\hat{z}_{lf}^{o,i}(t)$ to the long-run shocks extracted from those series, the response $\hat{z}_{mf}^{o,i}(t)$ to their medium-run shocks, and the response $\hat{z}_{hf}^{o,i}(t)$ to their short-run shocks. These shocks produce a change in the *Spread* if the correspondent parameters $\hat{\alpha}_j^{o,i}(t)$ of eq. (9) are significantly different from zero. The time it takes

Table 6: Pre-Turmoil Responses of the Spread to Long-Run Shocks

Spread (*Euribor-Eurepo spread with 3-month maturity*)			
	Asymptotic Final Effect (*basis points*)	Decay Time (*days*)	Initial Speed of Response (*bps per working day*)
MPR	4.58 (0.10)	216	0.06
MRO	-1.20E-04 (4.27E-06)	210	-1.71E-06
LTRO3m	-5.53E-05 (1.87E-06)	388	-4.28E-07
iTraxxSF	0.32 (0.03)	200	4.81E-03

This table in the first column reports the asymptotic final effect produced on the *Spread* in the pre-turmoil period by one unit of measure increases (maintained in time and not offset by any factor) in the long-run shocks stemming from the MPR, the MRO, the $LTRO3m$, and the $iTraxxFS$. The number in parentheses are twice the estimated standard deviations of the estimates. The second column shows the decay time it takes to reach the final asymptotic effects. The third column shows the daily changes, measured in basis points, in the spread during the first 20 percent of the decay time of the shocks.

for the *Spread* to respond to shocks depends on the parameters $\left(\hat{a}_j^{o,i}(t),\ \hat{b}_j^{o,i}(t)\right)$, *j=lf, mf, hf*, of eq. (8).

We evaluate the response of the *Spread* to the changes in the independent variables (as captured by the shocks) by means of step response functions, (as opposed to impulse response functions), because the ECB does not immediately undo the liquidity and policy measures it carries out. Given that the effects produced by the medium- and the short-run shocks are just temporary and tend to zero by construction, Table 6 presents only the responses by the *Spread* to the long-run shocks whose long-lasting, and possibly permanent, effects persist after the effects produced by the medium- and short-run shocks have faded away. In particular, Table 6 describes the response by the low-frequency component shares $\hat{z}_{lf}^{o,i}(t)$, for $t \to \infty$, of the *Spread*, to a one-unit-of-measure step increase applied to the long-run inputs $\hat{u}_{lf}^{i}(t)$ of the MPR, MRO, $LTRO3m$, and $iTraxxFS$. Given that it may take several months before the subsequent effects on $\hat{z}_{lf}^{o,i}(t)$ reach their final (asymptotic) values, it is unlikely that in the meantime no exogenous factor offsets, at least partly, their actions. Therefore, we also estimate the *Spread*'s immediate response to the long-run shocks. From the inception of the shocks to when they reach approximately 20 percent of their final asymptotic values, the step responses can be approximated with a linear function with a little margin of error. Then, in Table 6 we report also the initial speed of response, namely the estimate of the daily changes, expressed in basis points, of $\hat{z}_{lf}^{o,i}(t)$ during a period going from the inception of the shock to 20 percent of its decay time.

In the pre-turmoil period, an increase of one percentage point in the MPR, if not offset by any

exogenous factor, was expected to produce about a year after its inception (i.e. after 216 working days) a long-lasting increase of 4.58 basis points in the *Spread*. At the same time, an increase of EUR 10,000 millions in the liquidity allotted at the *LTRO3m,* if not offset by any exogenous factor, was expected to produce in about a year and a half (i.e. after 388 working days) a decline in the *Spread* of $(-5.53\text{E-}05 * 10,000) = -0.553$ basis points, whereas an increase of the same amount of the liquidity allotted at the *MRO,* if not offset by any exogenous factor, was expected to produce in about a year (i.e. after 210 working days) a decline in the *Spread* of -1.2 basis points. Finally, a one basis point increase in the *iTraxxFS* was expected to translate, if not offset by any exogenous factor, about a year later (i.e. after 200 working days) into a long-lasting increase in the *Spread* of 0.32 basis points.

The cumulative step responses to a one-unit-of-measure step increases in the long-, medium-, and short-run shocks due to rises in the *MPR*, *MRO*, and *LTRO3m*, and the *iTraxxFS* are plotted in Figure 4. The values taken by these step responses at the end of the horizon considered (1000 days) are those presented in Table 6, given that the responses to the medium- and short-run shocks fade away earlier than that.

Figure 5 shows the real-time estimates[19] of $z^{o,i}(t)$ of eq. (7), namely of the effects entailed on the *Spread* by the actual changes occurred in the pre-turmoil period in the independent variables (which have been decomposed into long-, medium-, and short-run shocks). Negative (positive) values on the y-axis of these graphs indicate that the changes in the related independent variable have produced a reduction (an increase) in the *Spread*.

In the pre-turmoil period, the ECB's separation principle whereby the pursued liquidity policy does not affect the stance set by monetary policy decisions, applied. In fact, graph (b) of Figure 5 shows that the contribution of the liquidity allotted at the *MRO* to the dynamics of the short-term Euribor-Eurepo spreads was on average close to zero. Graph (c) shows that the term liquidity allotted at the *LTRO3m* reduced the *Spread* by at most 1.7 basis points. These imply not only that the Euribor and the Eurepo reacted to injections of central bank money in essentially in the same measure, but also that the liquidity risk premium embedded in the Euribor was very small. The same consideration applies to the modest effect (of a 0.90 basis point increase on average) produced by the changes occurred in the *iTraxxFS* measuring the credit risk premium included in the Euribor. Graph (a) shows that in such environment, it took five consecutive increases in the *MPR*,[20] before in October 2006 the *Spread* began widening, thereby signaling that unsecured money market rates were affected more than secured money market rates by the higher cost of (central bank) refinancing. Yet, an overall increase of 150 basis points in *MPR* produced by end-February

[19] These are one-step ahead forecasts. Given that the parameters of the model have remained virtually unchanged during this period (3 October 2005 to 28 February 2007), and given the characteristic of the adopted filtering procedure, we denote these estimates *real time* estimates.

[20] The monetary policy rate was increased on 6 December 2005 from 2.00 percent up to 2.25 percent; on 8 March 2006 up to 2.50 percent; on 15 June 2006 up to 2.75 percent; on 9 August 2006 up to 3.00 percent; on 11 October 2006 up to 3.25 percent, and on 13 December 2006 up to 3.50 percent.

Figure 4: Pre-Turmoil Step Response Functions to the Rises in the Independent Variables

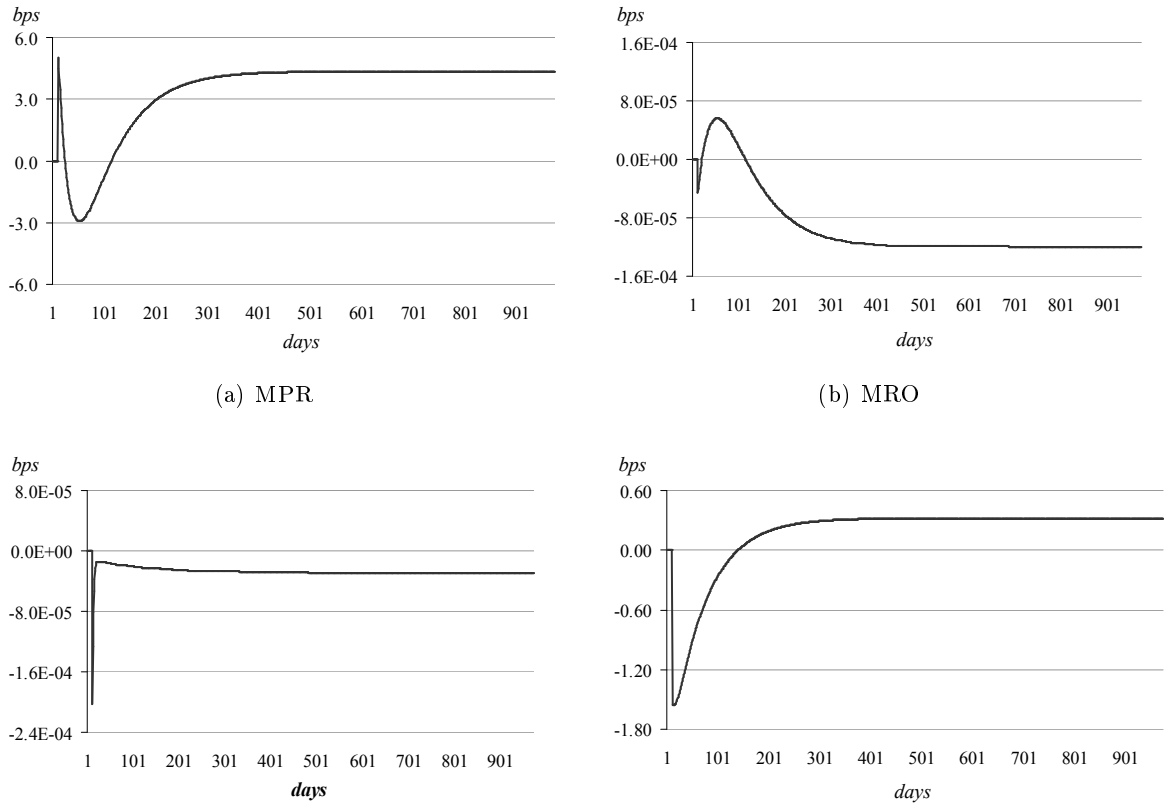

(a) MPR

(b) MRO

(c) LTRO3m

(d) iTraxxFS

These graphs show the cumulative step responses to a one unit of measure step increases in the long-, medium-, and short-run shocks stemming from changes in the MPR, the MRO, the $LTRO3m$, and the $iTraxxFS$ during the pre-turmoil period.

2007 a rise of only 2.5 basis points in the *Spread*.

Finally, Table 7 shows how relevant the considered independent variables have been in explaining the evolution of the *Spread* in the pre-turmoil period. The metric we use to gauge their contributions is the root mean square value, $RMSV = \sqrt{\frac{1}{368}\sum_{t=1}^{368}[\hat{z}^{o,m}(t)]^2}$, $m = o, i$ as in eq.eq. (7), expressed in basis points. We contrast the $RMSV$ of the contributions with the $RMSV$ of the variable being explained, namely the *Spread*, $RMSV = \sqrt{\frac{1}{368}\sum_{t=1}^{368}[\hat{z}^{o}(t)]^2}$, and we express the ratio between the two $RMSV$ in percent. Notice that the sum of the $RMSV$ of the contributions will not equal the $RMSV$ of the *Spread* whenever one or more explanatory variables caused a change in the *Spread* by reducing (or widening) it. Even though different explanatory variables may have pushed the risk premia embedded in the Euribor, as measured by the *Spread,* in different directions (up or downwards) hardly would they perfectly neutralize each other.

Table 7 shows that the residual, unknown, forces exerted by far the largest influence on the

Figure 5: Real-Time Estimates of the Effects Produced on the Spread Before the Turmoil

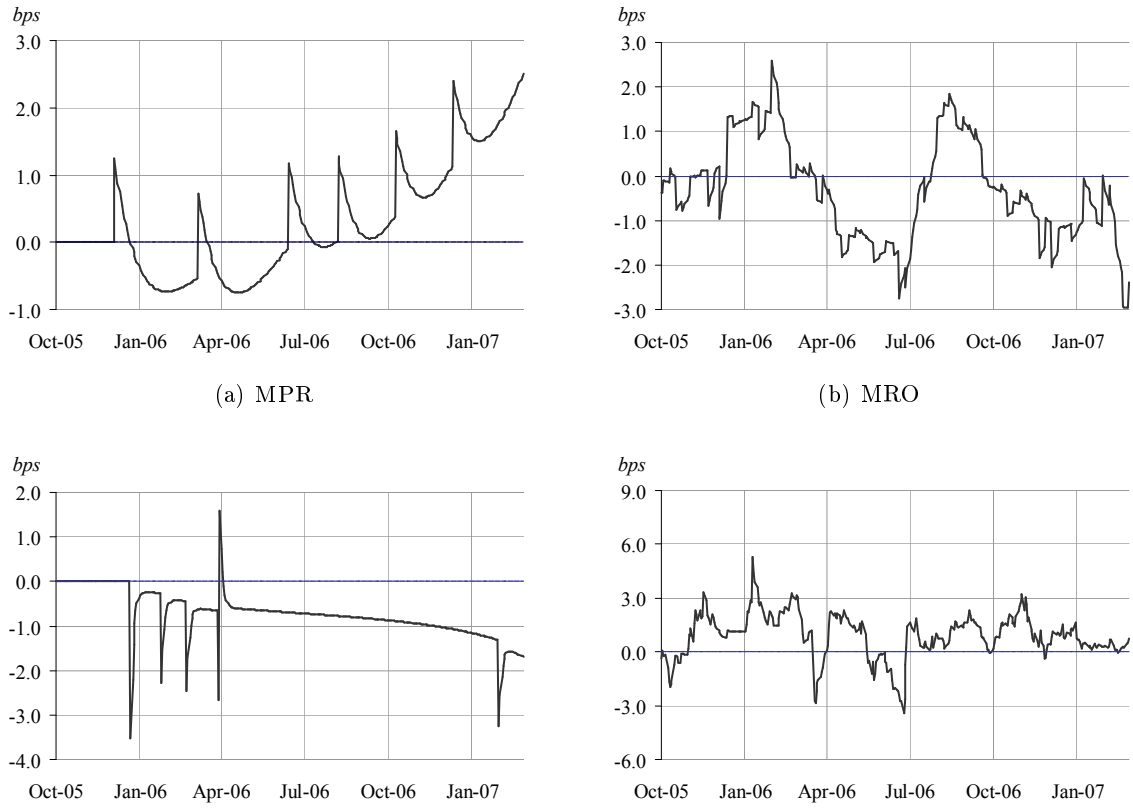

(a) MPR

(b) MRO

(c) LTRO3m

(d) iTraxxSF

These graphs show the real time estimates of the sum of the long-lasting, transitory and short-lived effects produced on the Euribor-Eurepo spread with 3-month maturity by the actual changes occurred in the MPR, MRO, $LTRO3m$, and $iTraxxFS$ over the period goes 3 October 2005 to 28 February 2007. Negative (positive) values on the y-axis of these graphs indicate that the changes in the considered variable have produced a reduction (an increase) in the spread.

dynamics of *Spread* in the pre-turmoil period. The changes in the *iTraxxFS* also mattered, probably because they helped explain the high-frequency changes describing almost entirely the behavior of the *Spread* before the eruption of the crisis. The *MRO* were the most relevant ECB's measure, whereas the *MPR* and the *LTRO3m* had a slightly less pronounced, yet significant, explanatory power.

7.3 The Change in the Model Parameters and the Rise in Risk Premia

The parameters of the model M^o can change over time, as explained in section 6. In particular, Figure 6 shows the evolution of the parameters $\alpha_{lf}^{o,i}(t)$ of eq. (9) measuring the long-lasting effect produced on the *Spread* (specifically, on its low-frequency component) by the long-run shocks

Table 7: Pre-Turmoil Contributions to the Evolution of the Spread

Spread (*Euribor-Eurepo spreads with 3-month maturity*)		
	Contribution to the RMSV	
	(*basis points*)	(*percent*)
MPR	0.91 (0.020)	12.50
MRO	1.17 (0.042)	16.03
LTRO3m	0.92 (0.031)	12.60
iTraxxSF	1.53 (0.148)	20.96
Residual	7.43 (0.464)	101.77

Note: The RMSV of the Spread = 7.30 bps

This table reports the root mean square values (RMSV) of the contributions to the dynamics of the *Spread* stemming from the changes actually occurred in the MPR, the MRO, the $LTRO3m$, the $iTraxxFS$, and the residual forces during the pre-turmoil period. The number in parentheses are twice the estimated standard deviations of the estimates. The second column shows the ratios, in percent, between the RMSV of the contributions and the RMSV of the *Spread*.

extracted from in i =*MPR, MRO, LTRO3m, iTraxxFS*. These parameters, which did not vary simultaneously,either exhibited a sudden and abrupt jump as in the case of the *iTraxxFS* and the *MRO*, or by displayed a smooth transition as in the case of the *LTRO3m*.

The seventh consecutive increase in the monetary policy rate level up to 3.75 percent, which the ECB carried out on 14 March 2007, triggered a rapid and sizable rise in the sensitivity of the Euribor to the progressively higher cost of refinancing at the ECB's tenders, as shown by the upwards shift in the parameter plotted in graph (a) of Figure 6, that by October 2007 moved to a level 8.85 times higher than in the pre-turmoil period. In the meantime, the ECB increased the monetary policy rate level to 4.00 percent (on 13 June 2007) and the turmoil officially began in the euro area (on 9 August 2007).

The parameter measuring the persistent effect of changes in the long-term liquidity allotted at the *LTRO3m* began to vary visibly in February 2007, reaching in December 2008 a level 16.75 times lower, as shown in graph (d) of Figure 6. Given that increases in central bank liquidity have a dampening effect on the *Spread*, the change in this parameter signals that euro area short-term unsecured money market rates grew extremely more responsive to term funding. The parameter measuring the long-run effects of changes in the liquidity weekly allotted with the *MRO* began varying in mid-August 2007 and it rapidly shifted by end-August 2007 to a new steady state level 2.80 times smaller.

Finally, the parameter measuring the long-lasting effect on the *Spread* produced by changes in

Figure 6: The Parameters Measuring the Long-Lasting Effects on the Spread

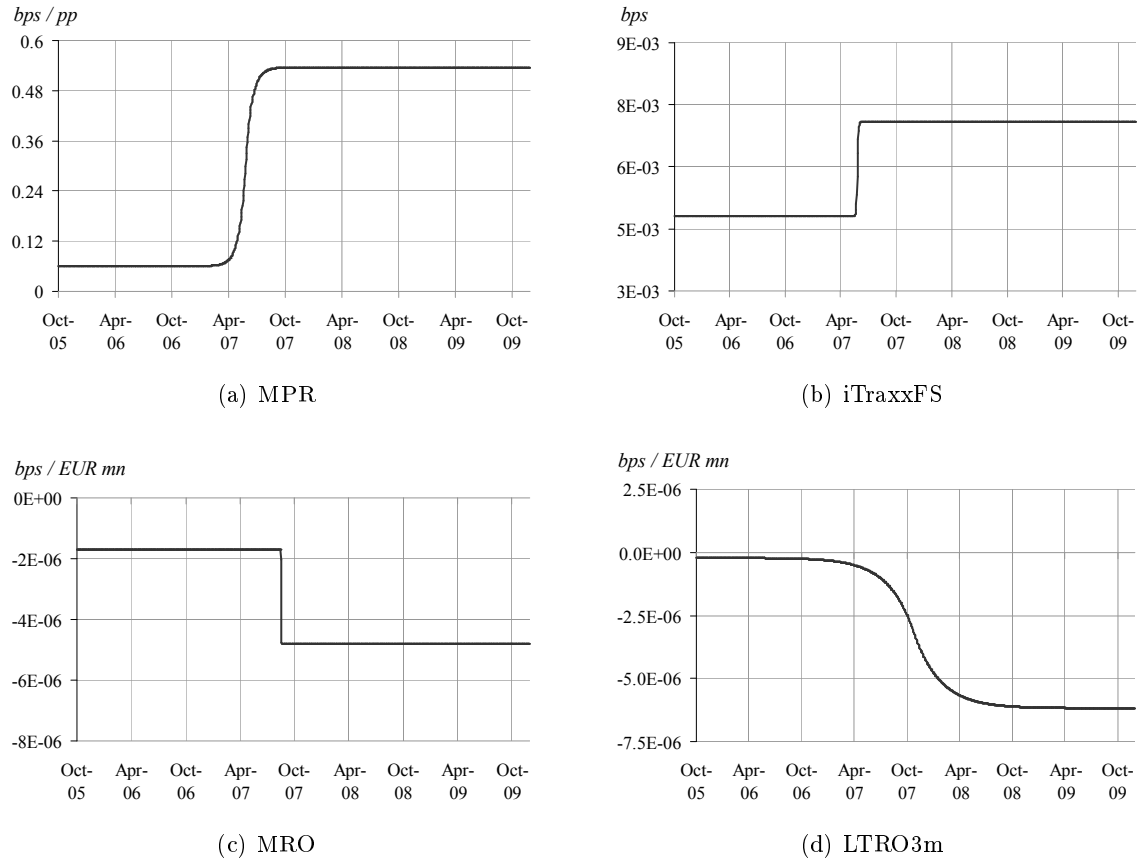

(a) MPR

(b) iTraxxFS

(c) MRO

(d) LTRO3m

These graphs show the evolution over the period 3 October 2005 - 30 November 2009 of the parameters $\alpha_{lf}^{o,i}(t)$ of the model M^o measuring the impact of the long-run shocks extracted from the MPR, the MRO, the $LTRO3m$, and the $iTraxxFS$ on the evolution of the Euribor-Eurepo spread with 3-month maturity.

the *iTraxxFS*, and thus in counterparty credit risk perceptions, started varying visibly in May 2007 reaching in July 2007 a new steady state level 1.48 times higher, as shown in graph (b) of Figure 6.

7.4 The Turmoil Period

In this section, we investigate the response of the *Spread* to the ECB's monetary and liquidity policy measures and to the changes in the *iTraxxFS* over the period 1 August 2007 to 30 November 2009 (609 observations).

Table 8 presents the responses by the *Spread* to a one-unit-of-measure step increase applied to the long-run shocks of *MPR*, *MRO*, *STRO*, *LTRO3m*, *LTRO6m1Y* and *iTraxxFS*. The comparison with the results reported in Table 6 reveals that during the turmoil, while surging to historical highs, the risk premia embedded in the Euribor have also grown much more responsive than in the past to the ECB's monetary and liquidity policy measures, although the time it takes for the liquidity

Table 8: Turmoil Period Responses of the Spread to Long-Run Shocks

Spread (*Euribor-Eurepo spreads with 3-month maturity*)			
	Asymptotic Final Effect (*basis points*)	Decay Time (*days*)	Initial Speed of Response (*bps per working day*)
MPR	39.30 (0.86)	220	0.54
MRO	-4.76E-03 (1.69E-04)	2987	-4.78E-06
STRO	-3.59E-04 (3.49E-05)	246	-4.39E-06
LTRO3m	-5.37E-04 (1.82E-05)	261	-6.17E-06
LTRO6m1Y	-5.87E-04 (1.62E-05)	485	-3.63E-06
iTraxxSF	2.35 (0.23)	993	0.01

This table in the first column reports the asymptotic final effect produced on the *Spread* in the turmoil period by one unit of measure increases (maintained in time and not offset by any factor) in the long-run shocks stemming from the MPR, the MRO, the $STRO$, the $LTRO3m$, the $LTRO6m1Y$, and the $iTraxxFS$. The number in parentheses are twice the estimated standard deviations of the estimates. The second column shows the decay time it takes to reach the final asymptotic effects. The third column shows the daily changes, measured in basis points, in the spread during the first 20 percent of the decay time of the shocks.

measures to fully exert their effect has also increased.

Specifically, Table 6 shows that after the eruption of the crisis a one percentage point rise in the *MPR*, if not offset by any exogenous factor, is expected to produce about a year after its inception (after 220 working days) a long-lasting increase of 39.3 basis points in the *Spread* (it was 4.58 basis points before the turmoil). At the same time, an increase of EUR 10,000 millions in the liquidity allotted at the *LTRO3m,* if not offset by any exogenous factor, is expected to produce in about a year (after 261 working days) a decline in the *Spread* of -5.37 basis points (it was -0.553 basis points before the turmoil), whereas an increase of the same amount of the liquidity allotted at the *MRO,* if not offset by any exogenous factor, is expected to produce a decline in the *Spread* of -47.6 basis points (it was 1.2 basis points before the turmoil), although the time of response to the changes in the *MRO* has grown sizeably. As a result, the *MRO* end up with producing a steady decline in the *Spread* as long as they are not offset by forces exerting an opposite effect, as clearly shown in graph (b) of Figure 7. The initial speed of response by the *Spread* after a rise in the liquidity allotted at the MRO has increased by 2.8 times compared with the pre-turmoil period. The concerns on counterparty credit risk as gauged by the *iTraxxFS* have also become both more important for the *Spread* and much slower to manifest than in the past. A one basis point increase in this index, if

not offset by any exogenous factor, is expected to be associated to a long-lasting increase in the *Spread* of 2.35 basis points, although also in this case the time of response has become very long suggesting that counterparty credit risk concerns keep on slowly widening the *Spread*, as shown in graph (f) of Figure 7. The initial speed of response of the *Spread* to changes in the *iTraxxFS* has increased 1.48 times compared with the pre-turmoil period.

The cumulative step responses to a one-unit-of-measure step increases in the long-, medium- and short-run shocks stemming from rises in the *MPR*, *MRO*, *STRO*, *LTRO3m*, *LTRO6m1Y*, and the *iTraxxFS* are plotted in Figure 7. The values taken by the step responses at the end of the considered horizon (1000 days) are those presented in Table 8, given that the responses to the medium- and short-run shocks in the meantime fade away.

The real-time estimates of the effects entailed on the *Spread* by the actual changes occurred in the considered independent variables during the period 3 October 2005 to 30 November 2009 are shown in Figure 8. Negative (positive) values on the y-axis of these graphs indicate that the changes in the independent variables have produced a reduction (an increase) in the *Spread*. Graph (a) shows that the successive increases in the *MPR* caused the *Spread* to rise visibly starting from May 2007 up to about 100 basis points in early December 2008. Further insights on the repercussions for the risk premia embedded in the Euribor of progressively higher cost of (central bank) refinancing can be found in the literature investigating the link between monetary policy, the perception of risk, and bank risk-taking.[21] The widening pressure exerted by the *MPR* on the *Spread* started to abate in mid-December 2008, and the successive rapid declines in the monetary policy rate level (from 4.25 percent to 1.00 percent) carried out by the ECB from mid-October 2008 to mid May 2009 began to actually narrowing the *Spread* in mid-July 2009. At the end of the period considered in this study, the MPR was reducing the *Spread* by about 30 basis points.

Graph (b) of Figure 8 shows that the liquidity lent at the weekly *MRO* has not been large enough to offset the liquidity risk widening the Euribor-Eurepo spread. As explained in section 2.1, in the first phase of the crisis, in order to maintain essentially unaltered the outstanding liquidity volumes, the ECB reduced the liquidity allotted at the *MRO* to increase the term liquidity allotted at the *LTRO3m*. As a result, the ability of the *MRO* to countervail the widening in the money market risk premia was undermined. After the ECB adopted the fixed rate and full allotment procedure with which it has lent to the euro area banks all the (collateralized) liquidity they have bid for, the *MRO* kept on not having any actual corrective effect on the *Spread*, because banks have preferred borrowing longer-term (as shown in graph (d) of Figure 1, the liquidity allotted at the *MRO* declined sharply from June 2009 with the inception of the *LTRO1Y*).

Graphs (c), (d) and (e) of Figure 8 show than the provision of central bank term liquidity largely contributed to narrow the liquidity premia inflating the *Spread*.

[21] See, e.g., Rajan (2005); Borio and Zhu (2007); Adrian and Shin (2009); Altunbas, Gambacorta, Marques-Ibanez (2009), and Dubecq, Mojon, Ragot (2009).

Figure 7: Turmoil Period Step Response Functions to the Changes in the Independent Variables

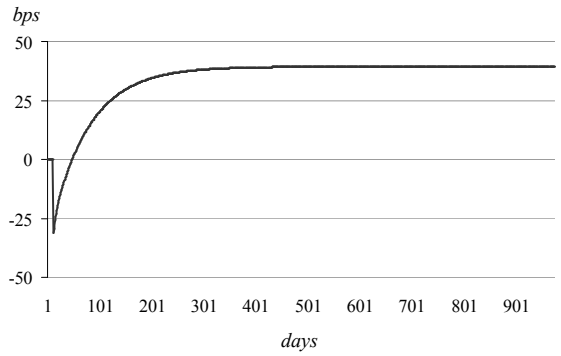

(a) MPR

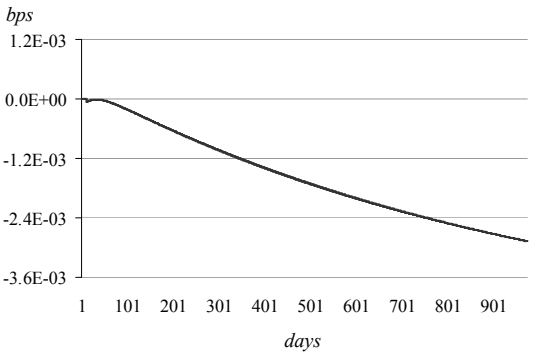

(b) MRO

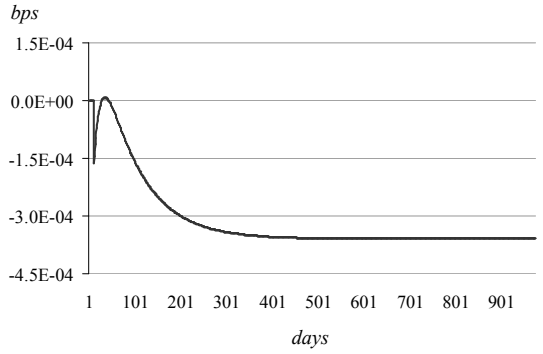

(c) STRO

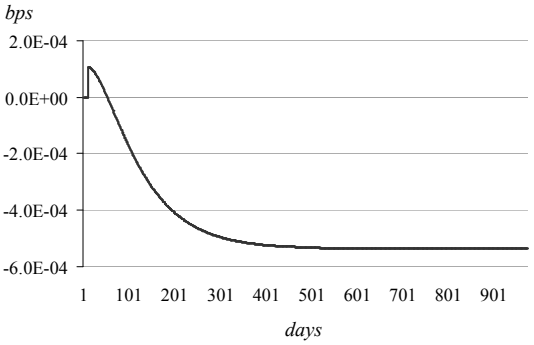

(d) LTRO3m

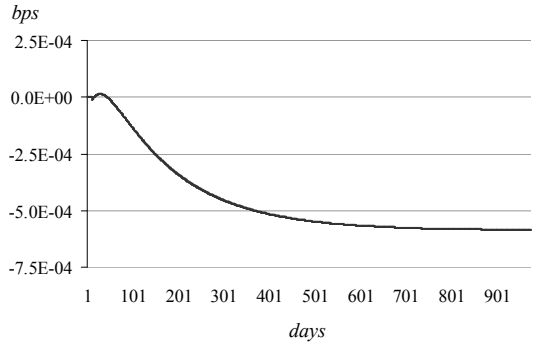

(e) LTRO6m1Y

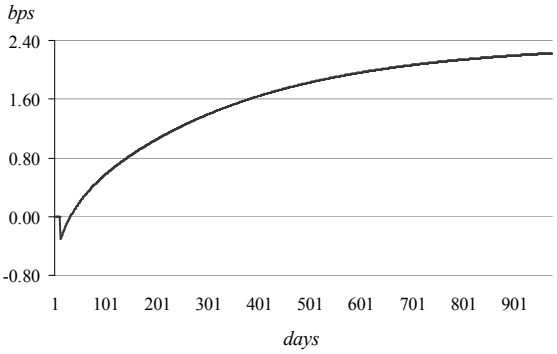

(f) iTraxxSF

These graphs show the cumulative step responses to a one unit of measure step increases in the long-, medium-, and short-run shocks stemming from changes in the MPR, the MRO, the $STRO$, the $LTRO3m$, the $LTRO6m1Y$, and the $iTraxxFS$ during the turmoil period.

Figure 8: Real-Time Estimates of the Effects Produced on the Spread During the Turmoil

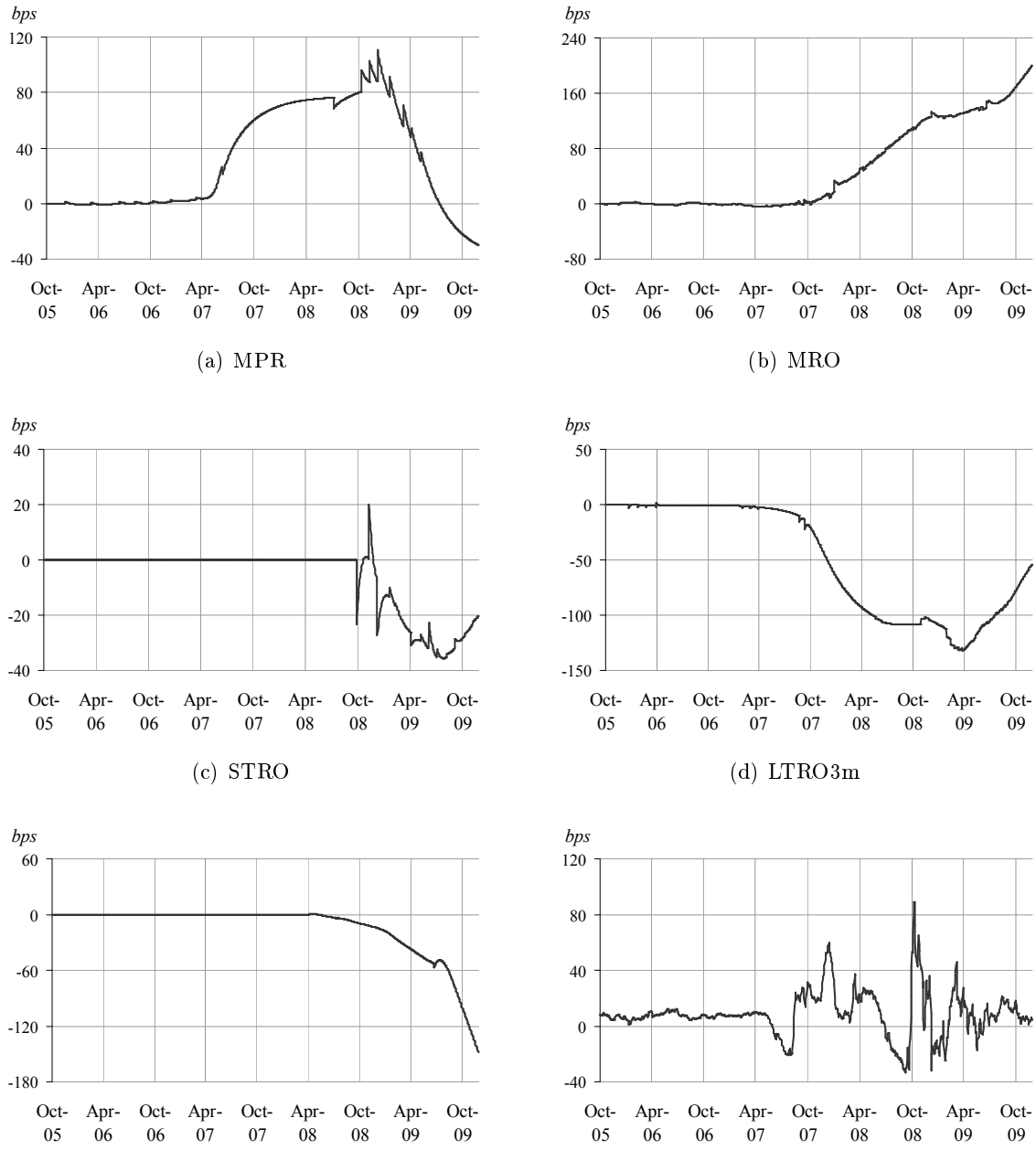

(a) MPR

(b) MRO

(c) STRO

(d) LTRO3m

(e) LTRO6m1Y

(f) Effect of the Residual Factors

These graphs show the real time estimates of the sum of the long-lasting, transitory and short-lived effects produced on the Euribor-Eurepo spread with 3-month maturity by the actual changes occurred in the MPR, MRO, $STRO$, $LTRO3m$, $LTRO6m1Y$, and the residual forces. The considered period goes from 3 October 2005 to 30 November 2009. Negative (positive) values on the y-axis of these graphs indicate that the changes in the considered variable have produced a reduction (an increase) in the spread.

In particular, the $STRO$ produced a correction which was as large as -36 basis points in July

2009. The *LTRO3m* reduced the *Spread* by as much as −131 basis points at the end of March 2009. Yet, also the corrective effect of these liquidity measures was tamed by the announcement, and subsequently by the inception, of the *LTRO1Y*. In fact, by the end of the period investigated in this paper the *LTRO6m1Y* were the liquidity measure reducing the *Spread* the most (by−148 basis points).

Given that the corrective effects entailed by the different liquidity measures partly offset each other, in graph (a) of Figure 9 we plot the real time estimate of the effect they produced on the *Spread* when considered altogether. The ECB's liquidity measures reduced the liquidity risk premia embedded in the Euribor by as much as −51 basis points at the end of December 2007 (when the *Spread* surged due to year-end liquidity concerns) and by −67 basis points in early April 2009. The counter-factual exercise presented in graph (b) of Figure 9, showing the pattern that the *Spread* would have taken in the absence of the liquidity allotted at the *MRO*, *STRO*, *LTRO3m*, and *LTRO6m1Y*, indicates that these measures have had an important corrective effect in taming the Euribor-Eurepo spread throughout the crisis. Their corrective effect was neutralized only in the period going from immediately after the filing for bankruptcy by Lehman Brothers to mid-December 2008. By the end of the period investigated in this paper, the ECB's liquidity measures were reducing the liquidity premia embedded in the Euribor by about 20 basis points.

Figure 9: The Effect of the ECB's Liquidity Measures on the Spread

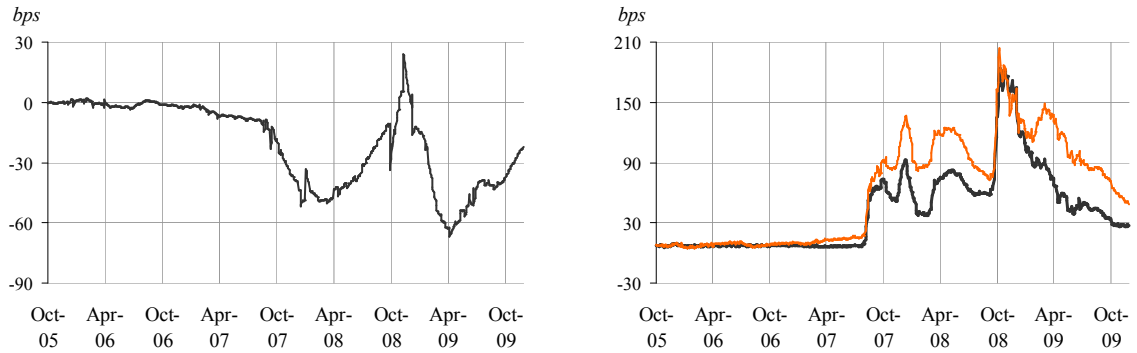

(a) (b)

Graph (a) shows the real time estimate of the cumulative effect produced on the Euribor-Eurepo spread with 3-month maturity by the liquidity allotted at the *MRO*, *STRO*, *LTRO3m*, and *LTRO6m1Y*. Graph (b) contrasts the actual short-term Euribor-Eurepo spread (dark line) with the pattern it would have taken in the absence of the liquidity measures (light line). Negative (positive) values on the y-axis of the graphs indicate that the changes in the liquidity measures have produced a reduction (an increase) in the spread. The considered period goes from 3 October 2005 to 30 November 2009.

Counterparty credit risk concerns as measured by the *iTraxxFS* have steadily increased their upward pressure on the *Spread*, as shown in graph (a) of Figure 10, consistently with their slowly evolving, yet persistent, nature. The counter-factual exercise presented in graph (b) of Figure 10,

showing the pattern that the *Spread* would have taken in the absence of the credit risk premium and in the absence of the correction entailed by the ECB's liquidity measures, indicates that while in the first phase of the turmoil the importance of the credit risk premium for the Euribor was modest compared with that of the liquidity risk premium, its weight has grown increasingly larger thereafter, especially in the course of 2009 when the ECB's liquidity measures successfully tamed the liquidity risk component of the *Spread*. In particular, graph (b) suggests that given the all measures taken by the EU fiscal and monetary authorities, by April 2009 the Euribor-Eurepo spread would have turned negative had not it been inflated by credit risk premia. Indeed, it is only starting from May 2009 that has the contribution of the credit risk premium to the *Spread* stabilized, at around a level of 80 basis points, and only in November 2009 has it shown some tentative sign of retreating. By the end of the period investigated in this paper, the counterparty credit risk premia was widening the Euribor by about 75 basis points.

Figure 10: The Effect of Credit Risk on the Spread

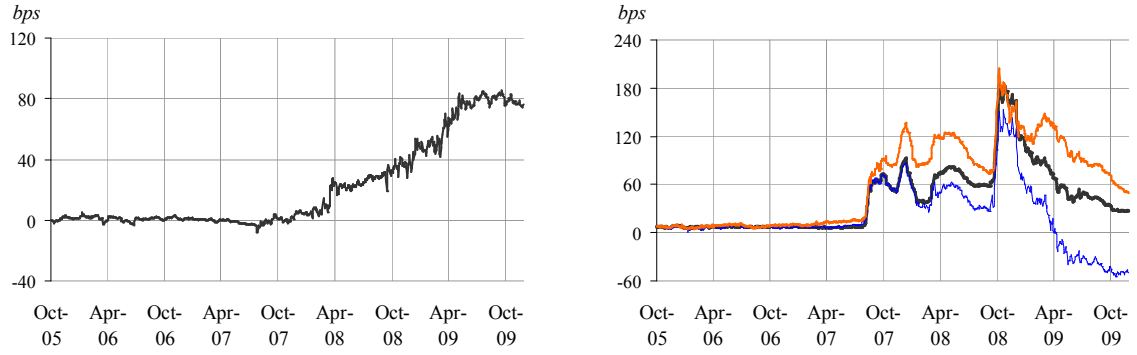

(a) Effect of the iTraxxFS

(b) Effect of Credit and Liquidity Risks

Graph (a) shows the real time estimate of the effects produced on the Euribor-Eurepo spread with 3-month maturity by the changes observed in the *iTraxxFS*. Graph (b) contrasts the actual short-term Euribor-Eurepo spread (thick dark line) with the pattern it would have taken in the absence of the credit risk premia measured from the *iTraxxFS* (thin lower line), and the pattern it would have taken in the absence of the liquidity measures (light higher line). Negative (positive) values on the y-axis of the graphs indicate that the changes in the credit risk premia have produced a reduction (an increase) in the spread. The considered period goes from 3 October 2005 to 30 November 2009.

Graph (b) of Figure 10 also shows that some movements of the *Spread* cannot be explained by the credit risk premium as measured by the *iTraxxFS*, and by the liquidity risk correction produced by the ECB's liquidity measures. The contribution to the *Spread* produced by the residual forces plotted in graph (f) of Figure 8 accounts for the missing explanations. The effects of the shocks captured by the residual forces have had systemic implications for the financial system. The most well-known and easily identifiable events from graph (f) occurred at the end of December 2007, at the moment of the sharp rise in the risk premia due to year-end banks' liquidity concerns, in March 2008 at the time of the rescue of Bear Sterns, in October and November 2008 in the wake of the

filing for bankruptcy by Lehman Brothers, and in the spring of 2009 when the deterioration in the economic outlook raised concerns for the industrialized economies. The less obvious information provided by the residual forces concerns the period before the eruption of the crisis, when their contribution to the *Spread* was negative, thereby signaling an underpricing of risk, at a moment in which the *Spread* should have instead widened following the increasingly higher cost of refinancing at the ECB's tenders. Brief periods of underpricing of risk occurred in reaction to the fiscal and monetary policy actions announced (and partly taken) in October 2008 and in the spring of 2009, thereby signaling that such measures have been crucial in restoring market participant's confidence. By the end of the period investigated in this paper, the systemic risk premium was widening the Euribor by only 4 basis points.

Table 9: Contributions to the Evolution of the Spread During the Turmoil

Spread (*Euribor-Eurepo spreads with 3-month maturity*)		
	Contribution to the RMSV	
	(*basis points*)	(*percent*)
MPR	64.22 (1.40)	82.54
MRO	108.34 (3.86)	139.26
STRO	17.46 (1.70)	22.44
LTRO3m	94.00 (3.18)	120.82
LTRO6m1Y	44.34 (1.22)	56.99
iTraxxSF	48.38 (4.68)	62.18
Residual	23.07 (1.44)	29.65

Note: The RMSV of the Spread = 77.80 basis points

This table reports the root mean square values (RMSV) of the contributions to the dynamics of the *Spread* stemming from the changes actually occurred during the turmoil period in the MPR, the MRO, the $STRO$, the $LTRO3m$, the $LTRO6m1Y$, the $iTraxxFS$, and the residual forces. The number in parentheses are twice the estimated standard deviations of the estimates. The second column shows the ratios, in percent, between the RMSV of the contributions and the RMSV of the *Spread*.

Finally, Table 9 shows how relevant the considered variables have been in explaining the evolution of the *Spread* in the turmoil period. The *MRO* have been the most relevant explanatory variable. This result is supported by the theoretical model proposed by Holthausen and Eisenschmidt (2009), which suggests that despite the introduction of operations with longer maturities, the liquidity

allotted at the weekly *MRO* should not become too small in order to avoid that interest rates rise when the prevailing conditions in the money market prevent troubled banks from financing their needs in the interbank market. The second most important variable has been the term liquidity allotted at the *LTRO3m*, followed by the *MPR*. The contributions of the *LTRO6m1Y* and of the *iTraxxFS* are much smaller, but noteworthy. Systemic risk concerns as measured by the residual forces and the *STRO* have been the measures contributing the least to the development in the risk premia embedded in the Euribor with a three-month maturity.

8 Conclusion

In this paper we propose a dynamic frequency decomposition approach to enhance our real-time understanding of the causes driving the risk premia embedded in the Euribor with a three month maturity. Our results indicate that the measures adopted by the ECB have effectively tamed the risk premia embedded in the Euribor, reducing to a small acceptable level the liquidity risk component, which accounted for the largest part of the premia at the beginning of the crisis. Also the importance of systemic risk, albeit still positive, has stabilized to a contained level since the spring of 2009. Instead, persistent and slowly evolving counterparty credit risk concerns have grown increasingly more important in the course of the turmoil, accounting for the largest share of the risk premia at the end of November 2009.

References

[1] Allen, F., Carletti, E., and D. Gale (2009), "Interbank Market Liquidity and Central Bank Intervention", forthcoming *Journal of Monetary Economics*.

[2] Altunbas Y., Gambacorta L., and D. Marques-Ibanez (2009) "Does Monetary Policy Affect Bank Risk-Taking?" mimeo.

[3] Artuç E. and S. Demiralp (2009) "Provision of Liquidity through the Primary Credit Facility during the Financial Crisis: A Structural Analysis" presented at the Federal Reserve Bank of New York Conference on 'Central Bank Liquidity Tools,' 19-20 February 2009.

[4] Borio C. and H. Zhu (2007) "Capital Regulation, Risk-Taking and Monetary Policy: A Missing Link in the Transmission Mechanism" Bank for International Settlements, Basle.

[5] Caballero R. J. and A. Krishnamurthy (2008) "Musical Chairs: A Comment on the Credit Crisis" Financial Stability Review, Special Issue on Liquidity, No. 11, Banque de France, 9-11.

[6] Cassola N. and C. Morana (2008) "Modeling Short-Term Interest Rates Spreads in the Euro Money Market" *International Journal of Central Banking*, 4:4, 1-37.

[7] Cecchetti S. G. and P. Disyatat (2009) "Central Bank Tools and Liquidity Shortages", prepared for the Federal Reserve Bank of New York Conference on 'Central Bank Liquidity Tools,' 19-20 February 2009.

[8] Chen C.-T. (1999) Linear System Theory and Design. Oxford University Press, New York.

[9] Christensen J. H. E., Lopez J. A., and G. D. Rudebusch (2009) "Do Central Bank Liquidity Operations Affect Interbank Lending Rates?" presented at the Federal Reserve Bank of New York Conference on 'Central Bank Liquidity Tools,' 19-20 February 2009.

[10] Clark, P. (1987) "The Cyclical Component of US Economic Activity," *Quarterly Journal of Economics*, Volume 102, pp. 797-814.

[11] Donati F. (1971) " Finite-Time Averaged Power Spectra" *IEEE Transaction on Information Theory*, vol. IT-17, January, 7-16.

[12] Donati P. and F. Donati (2008) " Modeling and Forecasting the Yield Curve under Model Uncertainty" ECB Working Paper n. 917.

[13] European Central Bank, (ECB), (2008) "The Eurosystem's Open Market Operations During the Recent Period of Financial Market Volatility" ECB Monthly Bulletin, May, 89-104.

[14] European Central Bank, (ECB), (2009) "The Implementation of Monetary Policy since August 2007" ECB Monthly Bulletin, July, 75-89.

[15] Eisenschmidt J. and J. Tapking (2009) "Liquidity Risk Premia in Unsecured Interbank Money Markets" ECB Working Paper n. 1025.

[16] Fleming M., Hrung W., and Keane F. (2009) "Repo Market Effects of the Term Securities Lending Facility" presented at the Federal Reserve Bank of New York Conference on 'Central Bank Liquidity Tools,' 19-20 February 2009.

[17] Harvey, A.. (1985) "Trends and Cycles in Macroeconomic Time Series," *Journal of Business and Economic Statistics*, Volume 3, pp. 216-27.

[18] Heider F., Hoerova M., and C. Holthausen (2009) "Liquidity Hoarding and Interbank Market Spreads: The Role of Counterparty Risk" presented at the Federal Reserve Bank of New York Conference on 'Central Bank Liquidity Tools,' 19-20 February 2009.

[19] Hördahl P. and M. R. King (2008) "Developments in Repo Markets During the Financial Turmoil" BIS Quarterly Review, December, 37-53.

[20] Kwan S. (2009) "Behavior of Libor in the Current Financial Crisis" FRBSF Economic Letters, Number 2009-04.

[21] McAndrews J., Sarkar A., and Z. Wang (2008) "The Effect of the Term Auction Facility on the London Inter-Bank Offered Rate" *Federal Reserve Bank of New York Staff Reports*, No. 335.

[22] Michaud F.-L. and C. Upper (2008) "What Drives Interbank Rates? Evidence from the Libor Panel" BIS Quarterly Review, March, 47-58.

[23] Nobili, S. (2009) "Liquidity Risk in Money Market Spreads", Banca d'Italia, mimeo.

[24] Perron P. and T. Wada (2009) "Let's Take a Break: Trends and Cycles in US Real GDP," *Journal of Monetary Economics*, Volume 56, pp. 749-65.

[25] Rajan R. G. (2005) "Has Financial Development Made the World Riskier?" NBER Working Paper 11728.

[26] Taylor J. B. and J. C. Williams (2009) "A Black Swan in the Money Market" *American Economic Journal: Macroeconomics*, 1, 1, 58-83.

[27] Trichet J.-C. (2009a) "The ECB's Enhanced Credit Support" keynote address delivered at the University of Munich, Munich, on 13 July 2009.

[28] Trichet J.-C. (2009b) "Credible Alertness Revisited" intervention at the symposium on 'Financial Stability and Macroeconomic Policy' sponsored by the Federal Reserve Bank of Kansas City, Jackson Hole, 22 August 2009.

[29] Watson, M. (1986) "Univariate Detrending Methods with Stochastic Trend," *Journal of Monetary Economics*, Volume 18, pp. 49-75.

Appendix I

Consider the discrete-time function $z(t)$ whose pattern we want to investigate in the frequency domain. The function $z(t)$ is a finite power sampled time function satisfying the condition $\lim_{N\to\infty} \frac{1}{2N} \sum_{t=-N}^{N} [z(t)]^2 = Pz < \infty$ where Pz is the mean power of $z(t)$. If the data sampling unit considered is one day the upper limit of the frequency domain is $f_{max} = 0.5\, cycles/day = \pi\, rad/day$. Given that the mean power Pz is finite, the function $z(t)$ is not Fourier transformable. In this case, if $z(t)$ follows an ergodic stationary process, Pz is distributed in the frequency domain with a power spectrum $\Phi(f)$, such that: $Pz = \int_0^{fmax} \Phi(f)\, df$. If $z(t)$ follows a nonstationary process like the economic time series we consider, the signal power is likely to be time-varying. In this case, as shown by Donati (1971), it is possible to define a *class* of time-varying power spectral functions $\varphi(f_i, t)$, where f_i, with $i \in (1, Nf)$, denotes the frequency values belonging to a finite set of Nf elements, with the following properties: 1) $pz(t) = \sum_{i=1}^{Nf} \varphi(f_i, t)$ is a "*locally time averaged*" instantaneous power obtained by a suitable smoothing of the signal instantaneous power $[z(t)]^2$, such that:

$Pz = \lim_{N\to\infty} \frac{1}{2N} \sum_{t=-N}^{N} pz(t)$; and 2)$\bar{\Phi}(f_i) = \lim_{N\to\infty} \frac{1}{2N} \sum_{t=-N}^{N} \varphi(f_i, t)$, is a "*locally frequency averaged*" power spectral value such that $Pz = \sum_{i=1}^{Nf} \bar{\Phi}(f_i)$. If the signal $z(t)$ is the realization of an ergodic stationary stochastic process, the power spectrum $\bar{\Phi}(f_i)$ corresponds to a "*locally frequency averaging*" of the stochastic process power spectrum $\Phi(f)$.

The elements $\varphi(f_i, t)$ of the time-varying power spectrum class are related to the criteria selected to perform the local averaging in the time and frequency domains. While different averaging criteria may be adopted, they should meet the following general rules: i) a weighted averaging approach must be applied, with the weighting function defined in such a way that the averaged value may be attributed (even roughly) to a *finite interval,* whose amplitude is denoted T when referring to the *time interval,* and Δf when referring to the *frequency interval*. The intervals of amplitudes T and Δf define the *finite resolution* of the performed averages. As a result, in the time domain, two values $\varphi(f_i, t_1)$ and $\varphi(f_i, t_2)$ cannot differ significantly if the time instant difference $\|t_2 - t_1\|$ is not significantly larger than T. Similarly, in the frequency domain, two values $\varphi(f_1, t)$ and $\varphi(f_2, t)$ cannot be significantly different if $\|f_2 - f_1\|$ is not significantly larger than Δf. Moreover, ii) the time-varying power spectral decomposition is possible only if adopting finite resolutions T and Δf such that $T \cdot \Delta f \gg 1$. Note that if we adopt the greatest time resolution $T = 1\ day$, which is equal to the sampling unit, the required frequency resolution is $\Delta f = fmax$. Therefore no spectral decomposition is possible. Similarly, if we adopt the greatest frequency resolution, which in this paper is $\Delta f = 1/1065$ *cycles/day* since our data extend to 1065 daily observations, then the required time resolution coincides with all the time interval (running from 3 October 2005 to 30 October 2009) and no time-varying power spectrum may be considered, but only the power spectrum of the power averaged over all the available time series data.

Having clarified the above conditions, for the purpose of the study carried out in this paper we decide to opt for a good resolution in the time domain and to accept a relatively low resolution in the frequency domain. As a result, we decompose the time series $z(t)$ in only four spectral components: a low-, a medium-, a high-frequency component and a residual decomposition error lying within a residual very high-frequency domain, which we do not investigate.

Appendix II

From the theory of dynamic systems with a state space representation (see e.g. Chen, 1999) we know that given the system outputs $z_j(t)$, $j = lf, mf, hf$, of SISO systems expressed in the canonical form of eqs. (2) and (3) it is possible to estimate the states $\mathbf{q}_j(t)$, which are not directly accessible to measurement, and to reconstruct the inputs $u_j(t)$, $j = lf, mf, hf$ by means other dynamic systems, namely low-, pass-band filters of the type known in the engineering literature as input-output state observers. To extract three frequency components with the correspondent shocks from the time series $z(t)$, we use three dynamic filters working simultaneously. A schematic representation of their recursions is provided in Figure 11. Specifically:

First, we extract the low-frequency component $z_{lf}(t)$ and the long-run shocks $u_{lf}(t)$ by processing $z(t)$ with an input-output state observer designed to work within the pre-selected low-frequency domain $[0 \div f_{lf}]$. The state observer (or state estimator) is obtained by applying a closed-loop feedback control to the system M_{lf} by means of the dynamic compensation system CC_{lf}, which is a SISO system of the $2^{nd}-$order like M_{lf}. As a result, the overall model used to explain and estimate $z_{lf}(t)$ and $u_{lf}(t)$ is a dynamic system of the $4^{th}-$order. We call this encompassing model the model of the state observer. Once extracted, the low-frequency component $z_{lf}(t)$ is subtracted from $z(t)$ obtaining the residual time series $e_{lf}(t)$, that is, $e_{lf}(t) = z(t) - z_{lf}(t)$.

Second, we extract the medium-frequency component $z_{mf}(t)$ and the medium-run forces $u_{mf}(t)$ by processing $e_{lf}(t)$ with an input-output state observer designed to work within the pre-selected low-frequency domain $[0 \div f_{mf}]$. Also in this case the observer is obtained by applying a closed-loop feedback control to the system M_{mf} by means of the $2^{nd}-$order, SISO, compensation system CC_{mf}. The medium-frequency component $z_{mf}(t)$ is then removed from $e_{lf}(t)$ obtaining the series $e_{mf}(t)$.

Figure 11: Dynamic Filter Recursions to Decompose $z(t)$

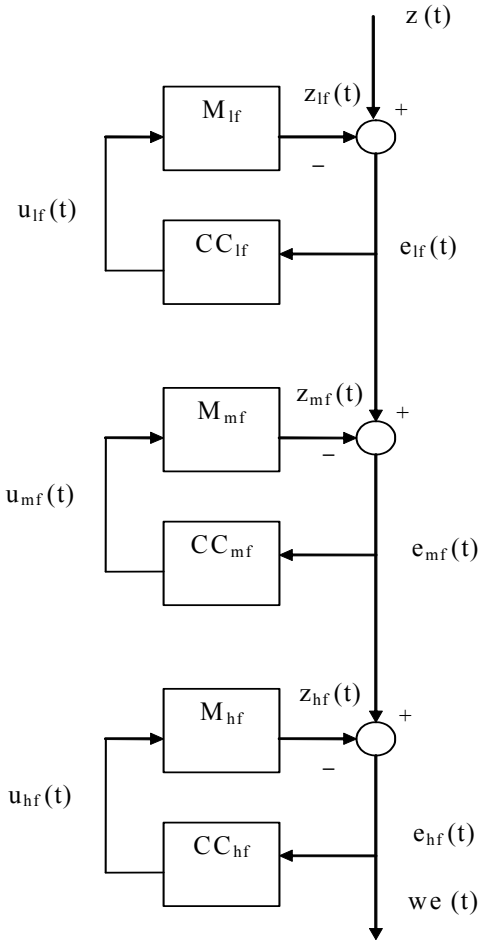

This graph shows the recursions of the dynamic filter carried out to perform the frequency decomposition of the generic time function $z(t)$.

Finally, we extract the high-frequency component $z_{hf}(t)$ and the short-run forces $u_{hf}(t)$ by processing $e_{mf}(t)$ with an input-output state observer designed to work within the pre-selected low-frequency domain $[0 \div f_{hf}]$. The state observer is obtained by applying a closed-loop feedback control to the system M_{hf} by means of the $2^{nd}-$order, SISO, compensation system CC_{hf}. The high-frequency component $z_{hf}(t)$ is then removed from $e_{mf}(t)$ obtaining the residual time series $we(t) = z(t) - z_{lf}(t) - z_{mf}(t) - z_{hf}(t)$ which lies within the residual frequency domain $[f_{hf} \div f_{max}]$. Given that $we(t) \to 0$ as $[f_{hf} \to f_{max}]$, by appropriately setting f_{hf} the residual series $we(t)$ is essentially noise.

As a result of the filter's reiterations described above, at each point in calendar-time t the sum of the three frequency components does not significantly differ from the actual value of $z(t)$, i.e. $z_{lf}(t)+z_{mf}(t)+z_{hf}(t) \cong z(t)$. In ensuring such outcome, the dynamic filter corrects for possible misspecifications of the models M_j and for the effects of measurement errors contained in $z(t)$.

We denote M the overall dynamic model of $z(t)$ including the three input-output state observers. Its

equations are:

$$\mathbf{q}(t+1) = \mathbf{H}\mathbf{q}(t) + \mathbf{B}z(t) \quad (13)$$

$$\mathbf{y}(t+1) = \mathbf{G}\mathbf{q}(t+1) \quad (14)$$

with eq. (13) the function $z(t)$ is decomposed into three frequency components using the (12×1) state vector $\mathbf{q}(t)$ – which includes the six state variables $\mathbf{q}_{lf}(t)$, $\mathbf{q}_{mf}(t)$ and $\mathbf{q}_{hf}(t)$ of the systems M_{lf}, M_{mf}, and M_{hf} and the state variables of the systems CC_{lf}, CC_{mf}, and CC_{hf} – the real, time-invariant (12×1) vector of parameters $\mathbf{B}$, and the real, time invariant (12×12) state transition matrix $\mathbf{H}$, which includes the state transition matrices of the systems M_j and CC_j for *j=lf, mf, hf.* With eq. (14) the real, time-invariant, (7×12) matrix $\mathbf{G}$ turns the state vector $\mathbf{q}(t+1)$ into the one-step-ahead forecast output vector $\mathbf{y}(t+1)$ with $\mathbf{y} \equiv \left[\begin{array}{cccccccc} u_{lf} & u_{mf} & u_{hf} & z_{lf} & z_{mf} & z_{hf} & \hat{z} \end{array} \right]$ where $\hat{z}(t+1)$ is the one-step ahead forecast of the function $z(t)$. Specifically, eq. (13) has the following representation:

$$\underbrace{\begin{bmatrix} q_{lf,1}(t+1) \\ q_{lf,2}(t+1) \\ q_{lf,3}(t+1) \\ q_{lf,4}(t+1) \\ q_{mf,1}(t+1) \\ q_{mf,2}(t+1) \\ q_{mf,3}(t+1) \\ q_{mf,4}(t+1) \\ q_{hf,1}(t+1) \\ q_{hf,2}(t+1) \\ q_{hf,3}(t+1) \\ q_{hf,4}(t+1) \end{bmatrix}}_{(12 \times 1)} = \underbrace{\mathbf{H}}_{(12 \times 12)} \underbrace{\begin{bmatrix} q_{lf,1}(t) \\ q_{lf,2}(t) \\ q_{lf,3}(t) \\ q_{lf,4}(t) \\ q_{mf,1}(t) \\ q_{mf,2}(t) \\ q_{mf,3}(t) \\ q_{mf,4}(t) \\ q_{hf,1}(t) \\ q_{hf,2}(t) \\ q_{hf,3}(t) \\ q_{hf,4}(t) \end{bmatrix}}_{(12 \times 1)} + \underbrace{\begin{bmatrix} 0 \\ 0 \\ d_{lf} \\ c_{lf} \\ 0 \\ 0 \\ d_{mf} \\ c_{mf} \\ 0 \\ 0 \\ d_{hf} \\ c_{hf} \end{bmatrix}}_{(12 \times 1)} z(t) \quad (15)$$

$$\mathbf{q}(t+1) = \mathbf{H}\mathbf{q}(t) + \mathbf{B}z(t)$$

with

$$\mathbf{H} = \begin{bmatrix} 1-a_{lf} & -b_{lf} & h_{lf} & k_{lf} & 0 & 0 & 0 & 0 & 0 & 0 & 0 & 0 \\ 1 & 1 & 0 & 0 & 0 & 0 & 0 & 0 & 0 & 0 & 0 & 0 \\ 0 & -d_{lf} & 1-r_{lf} & -s_{lf} & 0 & 0 & 0 & 0 & 0 & 0 & 0 & 0 \\ 0 & -c_{lf} & 1 & 1-c_{lf} & 0 & 0 & 0 & 0 & 0 & 0 & 0 & 0 \\ 0 & 0 & 0 & 0 & 1-a_{mf} & -b_{mf} & h_{mf} & k_{mf} & 0 & 0 & 0 & 0 \\ 0 & 0 & 0 & 0 & 1 & 1 & 0 & 0 & 0 & 0 & 0 & 0 \\ 0 & -d_{mf} & 0 & 0 & 0 & -d_{mf} & 1-r_{mf} & -s_{mf} & 0 & 0 & 0 & 0 \\ 0 & -c_{mf} & 0 & 0 & 0 & -c_{mf} & 1 & 1-c_{mf} & 0 & 0 & 0 & 0 \\ 0 & 0 & 0 & 0 & 0 & 0 & 0 & 0 & 1-a_{hf} & -b_{hf} & h_{hf} & k_{hf} \\ 0 & 0 & 0 & 0 & 0 & 0 & 0 & 0 & 1 & 1 & 0 & 0 \\ 0 & -d_{hf} & 0 & 0 & 0 & -d_{hf} & 0 & 0 & 0 & -d_{hf} & 1-r_{hf} & -s_{hf} \\ 0 & -c_{hf} & 0 & 0 & 0 & -c_{hf} & 0 & 0 & 0 & -c_{hf} & 1 & 1-c_{hf} \end{bmatrix}$$

and $r_j = a_j - h_j$ and $s_j = b_j + d_j - h_j$ for $j = lf, mf, hf$. The observation equation (14) has the following representation:

$$\underbrace{\begin{bmatrix} u_{lf}(t+1) \\ u_{mf}(t+1) \\ u_{hf}(t+1) \\ z_{lf}(t+1) \\ z_{mf}(t+1) \\ z_{hf}(t+1) \\ \hat{z}(t+1) \end{bmatrix}}_{} = \underbrace{\begin{bmatrix} 0 & 0 & h_{lf} & k_{lf} & 0 & 0 & 0 & 0 & 0 & 0 & 0 & 0 \\ 0 & 0 & 0 & 0 & 0 & 0 & h_{mf} & k_{mf} & 0 & 0 & 0 & 0 \\ 0 & 0 & 0 & 0 & 0 & 0 & 0 & 0 & 0 & 0 & h_{hf} & k_{hf} \\ 0 & 1 & 0 & 0 & 0 & 0 & 0 & 0 & 0 & 0 & 0 & 0 \\ 0 & 0 & 0 & 0 & 0 & 1 & 0 & 0 & 0 & 0 & 0 & 0 \\ 0 & 0 & 0 & 0 & 0 & 0 & 0 & 0 & 0 & 1 & 0 & 0 \\ 0 & 1 & 0 & 0 & 0 & 1 & 0 & 0 & 0 & 1 & 0 & 0 \end{bmatrix}}_{} \underbrace{\begin{bmatrix} q_{lf,1}(t+1) \\ q_{lf,2}(t+1) \\ q_{lf,3}(t+1) \\ q_{lf,4}(t+1) \\ q_{mf,1}(t+1) \\ q_{mf,2}(t+1) \\ q_{mf,3}(t+1) \\ q_{mf,4}(t+1) \\ q_{hf,1}(t+1) \\ q_{hf,2}(t+1) \\ q_{hf,3}(t+1) \\ q_{hf,4}(t+1) \end{bmatrix}}_{}$$

$$\begin{array}{ccc} (7 \times 1) & & (7 \times 12) & & (12 \times 1) \\ \mathbf{y}(t+1) & = & \mathbf{G} & & \mathbf{q}(t+1) \end{array} \tag{16}$$

The advantage of this filtering approach is that it allows us to exogenously set the eigenvalues of the matrix $\mathbf{H}$, which control the closed-loop dynamics of the three filters, because the $4^{th}-$order dynamic systems composing the state observers have four degrees of freedom each. Given that $\mathbf{H}$ is lower-triangular, the eigenvalues governing the dynamics of the filters are in its principal diagonal. We use 4 eigenvalues to extract and to model the evolution of each of the three frequency components in which decompose the time function $z(t)$. By exogenously setting the value of such eigenvalues we determine the parameters c_j, d_j, $h_j$and $k_j$of the matrix $\mathbf{H}$, while the remaining parameters a_j and b_j, for *j=lf, mf, hf*, are identified as described in section 4.4.

Given that the eigenvalues of the matrix $\mathbf{H}$ are the 12 roots p_k for $k = 1, \ldots, 12$ of the characteristic equation $det\,|p\mathbf{I} - \mathbf{H}| = 0$, by assigning to the eigenvalues the values specified in Table 1, we obtain the values of the parameters c_j, d_j, $h_j$and k_j for *j=lf, mf, hf*. Notice that the determinant of $\mathbf{H}$ is the product of the determinants of the three squared (4×4) submatrices lying in the principal diagonal of $\mathbf{H}$. Thus, the $12th-$order polynomial equation can be decomposed into three equations of the 4^{th} order. Given the specific property of these filters, each $4^{th}-$order equation can be further decomposed into the product of two equations of the 2^{nd} order, which are easy to solve. To solve the problem of the pole placement we have just described we use the algorithm included in the software suite EicasLab.

As shown in Table 1, in this study we impose the poles to be all real numbers. Moreover, we impose that the four values taken by each of the three poles be the same (e.g. all the poles used to extract the low-frequency component, p^i_{lf}, for $i = 1, \ldots, 4$ are set equal to 0.99).

Denote T the sampling period of $z(t)$, which in our case is one day ($T = 1$). Then, the value p_j (pure number) for *j=lf, mf, hf*, of the poles of the state observer used to extract the frequency component $z_j(t)$, is related to the upper bound f^{up}_j of the frequency bandwidth (measured in cycles/day) to which the frequency component $z_j(t)$ belongs, by the equation: $p_j = e^{-2\pi f^{up} T}$.

As explained above, the poles of the state observers are in one-to-one correspondence with the time-invariant parameters of the systems CC_j. These parameters characterize the step or impulse response of the observers, which are defined by the time constants τ_j for *j=lf, mf, hf*, representing the time it takes the response of each observer to reach about 63 percent of its final asymptotic value. The time constants τ_j of the state observers are related to the upper bound of the frequency bandwidths $f^{up}_j$by the relation $\tau_j = 1/2\pi f^{up}$. In this study, the time constants of the observers characterize also the persistence of the shocks $u_j(t)$ steering the dynamics of the models M_{lf}, M_{mf}, and M_{hf} of the frequency components of $z(t)$. We undertake that when a lapse of time corresponding to one time constant has passed from the inception of the shock $u_j(t)$, the effect produced by that force on the corresponding frequency component $z_j(t)$ has

become fully manifest.